July 2020

Gene Expression Regulation in the Mouse Liver by Mechanistic Target Of Rapamycin Complexes I and II

Anthony Poluyanoff

Gene expression regulation in the mouse liver by mechanistic target of rapamycin complexes I and II

A Thesis Presented

by

ANTHONY ALEXANDER POLUYANOFF

Submitted to the Graduate School of the
University of Massachusetts Amherst in partial fulfillment
of the requirements for the degree of

Master of Science

May 2020

Molecular and Cellular Biology

Gene expression regulation in the mouse liver by mechanistic target of rapamycin complexes I and II

A Thesis Presented

by

ANTHONY ALEXANDER POLUYANOFF

Approved as to style and content by:

_____
Alexander Suvorov, Chair

_____
J. Richard Pilsner, Member

_____
Laura N. Vandenberg, Member

_____
Scott C. Garman, Director, Molecular and Cellular Biology Program

ABSTRACT

GENE EXPRESSION REGULATION IN THE MOUSE LIVER BY MECHANISTIC TARGET OF RAPAMYCIN COMPLEXES I AND II

MAY 2020

ANTHONY ALEXANDER POLUYANOFF, B.S., UNIVERSITY OF MASSACHUSETTS, AMHERST

M.S., UNIVERSITY OF MASSACHUSETTS, AMHERST

Directed by: Professor Alexander Suvorov

The mechanistic target of rapamycin (mTOR) is a key serine/threonine protein kinase that functions in complexes mTORC1 and mTORC2. mTORC1, originally discovered due to its sensitivity towards the mTOR inhibitor rapamycin, responds to extracellular growth factor signaling, WNT signaling, and nutrient abundance via glucose and amino acid-triggered signaling. Downstream effectors of mTORC1 include autophagy, mitochondrial metabolic function, protein synthesis, and ribosome biogenesis. mTORC2, initially discovered as a rapamycin-insensitive complex of mTOR, responds to insulin, growth factor signaling, and inflammatory signaling such as tumor necrosis factor-alpha, with its downstream effectors being Akt, a key serine/threonine kinase that functions in cell division and is frequently dysregulated in many types of cancer, the NFkB pathway, and cytoskeletal reorganization and protein synthesis. Much research has been devoted to mTORC1 signaling, with mTORC2 receiving significantly less attention, despite both complexes' regulation of key cellular activities and response to rapamycin, as well as to other rapamycin-derived drugs (rapalogs). We have targeted both mTORC1 and mTORC2 for hepatocyte-specific deletion during the gestational period of mice, with the goal of describing mTORC1 and mTORC2 signaling and its perturbation in the adult mouse

hepatocyte. Our model has shown that deletion of RAPTOR, the regulatory associated protein of mTOR, and RICTOR, the rapamycin insensitive component of mTOR, in mTORC1 and mTORC2 respectively, leads to widespread effects on the hepatocyte transcriptome. We have found that a subset of genes responds both to Raptor and Rictor knockout, and an analysis of these genes indicates their function in key disorders of the liver, such as non-alcoholic fatty liver disease and hepatocellular carcinoma. Bioinformatic analysis following hepatocyte RNA sequencing of mTORC1 and mTORC2 knockout mice has revealed an unexpected upregulation of genes known to be regulated by these respective complexes. We have also found that cross talk exists between both complexes, in which the knockout of one yields the activation of the other. We have additionally found translationally relevant enrichments following Ingenuity Pathway Analysis (IPA) of RNA sequencing data. These results provide a key mechanistic discovery of mTOR signaling activity, and allow for a better understanding of the potential physiological effects of mTOR inhibition in human patients.

TABLE OF CONTENTS

Page

LIST OF TABLES

Table Page

LIST OF FIGURES

Figure Page

CHAPTER 1

INTRODUCTION

1.1 mTOR at a glance

The mammalian target of rapamycin (mTOR) is a key serine/threonine family kinase encoded in humans and other mammals, with significant and tight evolutionary conservation (1, 78). The association of mTOR with other proteins, forming mTOR complexes 1 (mTORC1) and 2 (mTORC2), initiates its associated signaling (1). mTORC1 signaling occurs following the binding of Raptor (regulatory protein associated with mTOR) with the HEAT domain of mTOR, and mLST8 (mammalian lethal with Sect13 protein 8) binding to the kinase domain of mTOR (79, 80, 81). mTORC1 signaling functions as a response to oxygen, growth factors, amino acids, and energy, with cellular stress serving as a well-characterized negative regulator of mTORC1 signaling (78). Common downstream effects of mTORC1 signaling include lipid and nucleotide synthesis, protein synthesis, and inhibition of autophagy, all serving to promote cellular growth (2, 78).

mTORC2, on the other hand, regulates different functions, and was originally discovered due to its insensitivity to rapamycin treatment, a mainstay inhibitor of mTORC1 (3). mTORC2 signaling occurs via the binding of Rictor (rapamycin-insensitive companion of mTOR) to the HEAT domain of mTOR, and mLST8 binding to the kinase domain of mTOR (3, 78). mTORC2 coordinates response to growth factor signaling, and its activation and downstream effectors positively regulate cell survival and cell proliferation (78). Specifically, mTORC2 is known to regulate Akt, a protein that is frequently dysregulated in particular cancers, and is also responsible for actin/cytoskeletal reorganization and protein synthesis (4). Recent basic and

translational research has indicated a role of mTOR in the development and progression of certain cancers, specifically in a model of hepatocellular carcinoma that demonstrated an increase in response towards the chemotherapeutic anti-metabolite 5-fluorouracil upon targeted silencing of mTORC1 and mTORC2 (5). Other works have demonstrated development of hepatocellular carcinoma in mice with chronic activation of mTORC1 that mirrors that of human hepatocellular carcinoma development (6). Additional research has elucidated that a specific anti-diabetic drug functions as a preventative measure for mTORC1-mediated liver injury via its inhibition of mTORC1 activity (7). Research has additionally focused on Non-Alcoholic Fatty Liver Disease (NAFLD), a common finding in the U.S population that affected 75-100 million Americans in 2017 (8). Recent work aimed to elucidate the pathogenesis of this syndrome has demonstrated that chronic inflammation promotes the progression of the disease, via increases in the low-density lipoprotein receptor and phosphorylation of mTOR (9). Besides these results, knowledge of the role of both mTORC1 and mTORC2 in regulation of hepatocyte gene expression remains limited.

1.2 The most comprehensive liver specific mTORC2 knockout study

One of the two most comprehensive studies on the effects of mTOR perturbation was conducted by Lamming et.al. in 2013. Rictor was knocked out using a LoxP/LoxP Albumin-cre mouse model. (10). To activate mTOR signaling, mice were unfed overnight for a total of 16 hours, and then allowed food *ad libitum* for three hours prior to sacrifice. To identify effects attributable to mTORC2 on the hepatic transcriptome, liver extracted from the Rictor KO group was compared to liver from wild-type mice (n=4). The comparison was achieved using microarray analysis on Affymetrix Genechip Mouse Gene 1.0 ST arrays (10), with a False Discovery Rate (FDR) q-value of less than 0.05 showing expression differences in a total of four

genes between control and Rictor KO (RKO) animals. These genes were the leptin receptor (Lepr), insulin-like growth factor binding protein 1 (Igfbp1), and the insulin receptor substrate 2 (Irs2), all strongly upregulated in RKO animals, with glucokinase downregulated in RKO animals(10). In order to confirm that these results were cell autonomous (not due to perturbed hormone or nutrient signaling), primary hepatocytes from RKO and WT were cultured and harvested for RNA, which yielded concordant increases in expression of Lepr, Igfbp1, and Irs2, in RKO cultures as compared to WT. Decreased Gck expression in RKO cultures was observed as concordant to decreased expression in RKO mouse liver samples as compared to WT. The aforementioned genes are all critical in both cell division and in lipid balance, suggesting a role for mTORC2 in regulation of lipid metabolism in the liver.

In addition, the Lamming et.al. study used mice that were unfed overnight for 16 hours, and then treated with 10-mg/kg rapamycin during feeding in order to inactivate mTORC1. This was conducted in order to compare the effects of mTORC2 KO with the effects of mTORC1 inhibition. This would therefore allow determination of complex-specific changes in hepatic gene transcription. Rapamycin administration was additionally decided upon in order to limit the activation of mTORC1-related genes that had been noted in a previous experiment (64). The liver transcriptome of rapamycin-fed animals was compared to the mTORC2 Rictor KO group using a microarray as was done for WT and Rictor KO mice in the previous experiment described. Changes in genes involved in the metabolism and synthesis of cholesterol, as well as changes in aldosterone signaling were all observed in rapamycin-treated mice as compared to Rictor KO mice (10). Aldosterone is the key human mineralocorticoid, synthesized from cholesterol, and functions as the effector molecule in the renin-angiotensin-aldosterone system. This system is critical in the regulation of blood pressure, fluid balance, and blood pressure (83).

Notably, no common biological functions or pathways were identified between Rictor KO mice and mTORC1 perturbed mice, with the only similarities being three transcription factors significantly altered in Rictor KO mice also altered in mTORC1 perturbed mice. This allowed for a generalized view of both mTORC1 and mTORC2 signaling, with the results indicating dissimilar downstream targets for both complexes.

Given that the role of mTOR in both complexes is to phosphorylate and activate downstream targets, RKO mice were analyzed with respect to their phosphoproteome as well (10). Three control mice and three RKO mice were unfed for 24 hours, and rapamycin was administered 10-mg/kg for both groups one hour prior to *ad libitum* access to food, in order to eliminate mTORC1-dependent signaling that had been observed in a previous experiment (64). Mice were euthanized 45 minutes into the refeeding period, and liver samples were analyzed using a western immunoblot. Results showed reduced AKT phosphorylation, as well as reduced PKCα phosphorylation, consistent with selective mTORC2 depletion, with reduction of S6K phosphorylation confirming mTORC1 inhibition by rapamycin (10). To explore if known mTORC1-regulated sites were changed in RKO mice, the above data was compared to a previous analysis of rapamycin treatment in mice (64) and to a quantitative analysis of rapamycin-sensitive sites in cell lines (65). Results showed that of 144 RKO-associated proteins characterized in the current experiment, only one, CAD S1859, an S6K substrate, was previously noted as either rapamycin sensitive or mTORC1 regulated (10).

In summary, these results showed a detailed view of mTORC2 signaling, indicating that the role of mTORC2 in hepatic signaling is complex, and that its effects are not observed to overlap significantly with mTORC1.

1.3 The most comprehensive liver-specific mTORC1 study

The most comprehensive research on mTORC1 signaling in the mouse liver comes from Boylan et. al. in 2015. The study design utilized three groups in total, all composed from Sprague-Dawley rats: fetal rats, non-proliferating adult rats, and proliferating rats. Fetal rats were administered rapamycin via intraperitoneal injection *in-situ* on embryonic day 19 at a dose of 5 micrograms and sacrificed on embryonic day 20. Non-proliferating adults (adults whose livers were not partially resected) were fasted for 48 hours, fed, and sacrificed 3 hours post re-feeding. Proliferating adults underwent a 2/3 hepatectomy and were sacrificed 24 hours later. Rapamycin was administered as a peritoneal injection at a dose of 250 micrograms per 100 g body weight 15 minutes before re-feeding of non-proliferating adults, and one hour before the 2/3 hepatectomy on proliferating adults. Analysis of transcriptome product was accomplished by a microarray on the Affymetrix Genechip Rat Gene ST 1.0 and Gene Set Enrichment Analysis.

Initial characterization of rapamycin inhibition of mTORC1 signaling yielded marked, but incomplete, inhibition of S6 phosphorylation. The effect on the mTOR target 4E-BP1 was described as significant but small in magnitude, indicating that rapamycin achieves incomplete inhibition of mTOR1 signaling in the context of the Sprague-Dawley rat experimental model (1).

Transcriptome (RNA product) analysis via Gene Set Enrichment Analysis (GSEA) for the three groups indicated discordant activity: non-proliferating adult rats treated with rapamycin exhibited a strong upregulation of genes involved in oxidative phosphorylation, with only splicesome-associated genes being downregulated. Proliferating rats, induced via the 2/3 hepatectomy as described above, exhibited an induction of lysosomal metabolism, steroid metabolism, and the acute phase response of the immune system, with no KEGG (Kyoto encyclopedia of genes and genomes) results yielding downregulation that was statistically

significant. Interestingly, fetal rats administered rapamycin exhibited a downregulation of lysosomal genes that were upregulated in adult non-proliferating rats. Indeed, fetal rats exhibited downregulation in contrast to upregulation for all of the most significantly affected gene sets for both non-proliferating and proliferating rats.

Analysis of the translatome (protein product) initially showed no changes in polysomes for fetal and adult rats treated with rapamycin, and microarray analysis did not show separations between rapamycin and control DMSO liver samples, indicating that the effects of rapamycin were likely on a small subset of genes. Translational efficiency calculations noted that for non-proliferating rats, rapamycin administration induced a moderate decrease in translational efficiency, while for proliferating adult rats translational efficiency did not change. Fetal rats, on the other hand, exhibited a marked increase in translational efficiency upon rapamycin treatment, with a total of 53 genes increased that showed an overall dominance of chemokine ligands and acute-phase reactants (1). Translational efficiency calculations for fetal rats, however, showed a resistance to rapamycin for the translation of genes with a complex 5' untranslated region, in direct contrast to both adult models, which exhibited rapamycin-mediated inhibition of translational activity of complex 5' UTR genes (1).

Overall, the Boylan et. al study notes that there is a significant discord between mTORC1 signaling in the fetal as compared to the adult liver, with additional discord displayed between a non-proliferating and proliferating adult liver. Fetal rats are observed to have a more rapamycin-resistant phenotype than adult rats, while rapamycin treatment of non-proliferating and proliferating animals induced the expression of different genes between groups. This leads to the conclusion that mTORC1 activity is not consistent throughout development, and that differences also arise in its activity in proliferating and non-proliferating liver tissue. The rapamycin

resistance observed in fetal rats was described as a possible mechanistic explanation to rapamycin resistance observed in certain cancers. Specifically, it was noted that the asynchronous proliferation in the rat fetus represented a cellular condition observed in many cancer cells, which could theoretically explain rapamycin resistance in certain cancers. In summary, the most notable conclusion from this work revolved around a clear developmental and physiologically divergent effect of mTORC1 signaling during different developmental and proliferative stages of the rat hepatocyte.

1.4 A summary of the two key liver specific mTOR knockout studies

The above two studies serve as the most recent liver-specific study of mTORC1 and mTORC2 signaling perturbations, and with the incorporation of next-generation sequencing, allow for visualization of the downstream effects of perturbation in both signaling complexes. However, there exists research suggesting a close signaling and regulatory relationship between mTORC1 and mTORC2 (11), and taking into account the works of Lamming et. al. and Boylan et. al., there still remains a gap in the knowledge of downstream effects of either mTORC1 or mTORC2 perturbation, specifically in regards to a pure knockout in contrast to administration of rapamycin to achieve mTORC1 inhibition.

1.5 An overview of mTOR signaling

It is known that high cellular energy and growth factor signaling serves as an activator of mTORC1 signaling through its positive regulation of PI3K and IRS. This in turn allows for AKT activation, which activates mTORC1 via an inhibition of the TSC1/TSC2 complex, allowing for RHEB-mediated activation of mTORC1 signaling (46-49). mTORC1 signaling then upregulates S6K1, which inhibits PI3K and thus negatively regulates AKT signaling, providing negative feedback to mTORC1 activation (49).

While mTORC2 activation is not as well studied (11), it is known that PI3K activation via growth factor signaling allows for a catalysis of PIP2 to PIP3, with PIP3 then activating mTORC2. Given that mTORC1 activation yields S6K1 transcription, which then negatively regulates PI3K, inhibition of mTORC1 may have downstream effects on mTORC2, mechanistically occurring via the loss of S6K1 negative regulation of PI3K, thus allowing for PIP3-mediated activation of mTORC2 signaling (51-53). Recent research has highlighted the role of PI3K in activation of mTORC2, specifically that AKT-independent activation of mTORC2 is dependent on PI3K-mediated conversion of PIP2 into PIP3 (12). Earlier research additionally established that PIP3 was capable of inducing mTORC2 signaling in cell cultures characterized by an AKT knockout phenotype (13). These studies have raised questions on the regulation of mTORC1 and mTORC2 signaling and subsequent transcriptome-wide effects, and have led us to pursue an experimental design allowing for comparison of gene expression in mice that have either mTORC1 *or* mTORC2 knocked out *in utero.*

1.6 Our experimental approach

Recent discoveries have noted that mTORC1 signaling changes with age (54). Specifically, it was noted that mTORC1 signaling, as measured by the activity of well-characterized targets of mTORC1 activity, decreases with age in hepatocytes. In addition, it was found that mTORC2 signaling in unfed male mice increases with age (54). Given that mTORC1 responds to growth signaling and is a known regulator of cell division and division-critical downstream events, studies conducted with immature mice may show effects that are due to a baseline higher level of mTORC1 signaling, one that is not normally present in the adult population. To that end, we have chosen a model that utilizes fully developed adult mice, to present a view of mTORC1 and mTORC2 signaling that is not perturbed due to developmentally related events. This approach,

in contrast to the recent approaches taken by Lamming et. al. and Boylan et. al., allows for a clean comparison between mTORC1 KO and mTORC2 KO mice, with complete inhibition of either signaling complex via Raptor or Rictor knockout achieved during the early stages of gestation. This serves to mitigate any of the aforementioned developmentally related changes in signaling from affecting the hepatic transcriptome. In addition, this also avoids comparing a knockout model to a drug-induced suppression model, thereby maintaining more readily comparable data sets and results of mTOR signaling perturbation.

Our current work seeks to completely describe the role of mTORC1 and mTORC2 in the adult liver metabolism, and to evaluate the effects of knockout on gene expression in adult mouse hepatocytes. To our knowledge, studies comparing the effects of knockout of mTORC1 and mTORC2 specifically in mature mouse hepatocytes have not been conducted with a next-generation sequencing approach, making our work particularly relevant in understanding the role of both mTOR complexes in hepatocytes, particularly for genes that may have been missed with previous, non high-throughput analysis. With the evidence presented by the Lamming et. al and Boylan et. al studies indicating that there may not much crosstalk between the two complexes, we have identified the need to compare mTORC1 KO and mTORC2 KO animals directly, with a liver-focused RNA-seq approach to test if this is truly the case.

Our present study has found that there are significant differences in gene expression in mice with mTORC1 or mTORC2 knocked out, with a particular subset of genes found to be altered both in C1 and C2 KO animals. Indeed, a subset of Kegg, Reactome, and Gene ontology identities was upregulated both in response to mTORC1 KO and mTORC2 KO, indicating a compensatory response from either complex when one or the other is knocked out. We have additionally found several unique transcription factors, deemed upstream regulators, which are

predicted to be affected by an mTORC1 or mTORC2 KO genotype based on Ingenuity Pathway Analysis. These factors allow for us to create a more detailed map of hepatic mTOR signaling, and additionally allow for us to make certain translational connections between perturbations in mTOR signaling and the progression of hepatocellular carcinoma and non-alcoholic fatty liver disease. Together, these results add significant levels of detail to hepatic mTOR signaling, elucidate potential clinical implications of mTOR perturbations in the liver, and may explain the molecular mechanisms behind hepatocellular carcinoma and non-alcoholic fatty liver disease.

CHAPTER 2

MATERIALS AND METHODS

2.1 Mus. musculus model development

mTORC1 KO mice were generated by crossing Alb-cre females (Stock No: 003574, The Jackson Laboratories) with homozygous floxed mutant mice with LoxP sites flanking exon 6 of the Raptor gene (Stock No: 013188, The Jackson Laboratories). The resultant F1 offspring were heterozygous for the Raptor flox allele and the albumin-cre transgene. These F1 females were then backcrossed with Raptor floxed males, and the offspring F2 generation were genotyped with qRT-PCR to identify F2 offspring homozygous for floxed Raptor and heterozygous for Alb-cre transgene, with approximately 25% of the F2 generation yielding this genotype. mTORC2 KO via Rictor KO were generated utilizing an identical protocol, with the only difference being in the first cross, where mice possessing homozygous LoxP sites flanking exon 11 of the targeted Rictor gene (Stock No: 020649, The Jackson Laboratories) were used.

Following development of the F2 generation, the offspring, hereafter referenced as the F3 generation, were allowed to develop for 75 days postnatal, and were then euthanized. These animals were homozygous for Rictor and raptor deletion, with WT animals lacking Alb-cre transgene on the floxed Rictor/raptor sites. Livers of these animals were excised, and following completion of liver excision, small samples of the livers of these euthanized animals were taken for RNA sequencing. The remaining liver samples were frozen at -81 centigrade storage for future analysis.

2.2 RNA Extraction

RNA extraction was conducted using approximately 1.0 gram of thawed liver tissue homogenized with 1.0 mL of TRIzol reagent (ThermoFischer Catalog No: 15596026). The homogenized solution was phase separated in 0.2 mL of isoamyl-free chloroform, vortexed, and centrifuged at 12,000g for 15 minutes at 4 degrees centigrade. The aqueous layer present in the centrifuged tubes was transferred to new centrifuge tubes, mixed with 0.5 mL of isopropyl alcohol, and centrifuged at 12,000g under 4 degree centigrade refrigeration to precipitate the RNA. Following centrifugation, the supernatant was removed and discarded, and two cycles of washing with 75% ethanol were conducted in a ratio of 1 mL ethanol:1 mL TRIzol reagent. Following the second wash with ethanol, the RNA precipitate was re-suspended in 100 microliters of Tris/Borate/EDTA (TBE) buffer, incubated at room temperature for 10 minutes, and analyzed for concentration and purity in a Nano-Drop spectrophotometer (Thermo-Fischer Catalog No: ND-2000). RNA quality was assessed using an Agilent 2100 Bioanalyzer (Agilent Technologies, Santa Clara, CA). All RNA samples were stored at -81 centigrade for further downstream analysis.

2.3 RNA-Seq Library Preparation

The plate was removed from -20 degree centigrade storage and thawed to room temperature, upon which 2.5 microliters of Resuspension buffer was added to each well plate, along with 12.5 microliters of A-Tailing Mix. The plate was run on the Bio-Rad CFX384 cycler at 37 degrees centigrade for 30 minutes and 70 degrees centigrade for five minutes.

To each well was added one unique RNA adapter index, along with 2.5 microliters each of Resuspension buffer and Ligation mix. The well plate was run at 30 degrees centigrade for one hour in the Bio-Rad CFX384 cycler. Upon completion, 5 microliters of the Stop Ligation Buffer was added to each well plate immediately.

42 microliters of AMPure XP beads were added to each well plate, and incubated at room temperature for 15 minutes. The plate was then placed on the magnetic stand for five minutes, and the supernatant was discarded. 200 microliters of 80% ethanol was added to each well and removed following 30-second incubation. This was repeated for a total of two washes. The plate was then allowed to dry on the magnetic stand for 15 minutes, upon which the plate was removed from the stand and to it was added 52.5 microliters of Resuspension Buffer. The plate was incubated for two minutes, placed on the magnetic stand for five minutes, and the 50 microliter supernatant from each well plate was transferred to a new well plate. To this was added 50 microliters of AMPure XP Beads, upon which the plate was incubated for 15 minutes and for a further five minutes on the magnetic stand. The supernatant was removed, and 200 microliters of 80% ethanol was used for two washes as described above. Following washing, 22.5 microliters of Resuspension Buffer was added to each well plate, the plate was incubated on the magnetic stand for five minutes, and the 20 microliters of the supernatant from each well was transferred to a new well of the plate.

Five microliters of PCR Primer Cocktail were added to each well with the supernatant, along with 25 microliters of the PCR Master Mix. The plate was run in the Bio-Rad CFX384 cycler for one cycle at 98 degrees centigrade for 30 seconds, 15 cycles at 98 degrees centigrade for 10 seconds, 60 degrees centigrade for 30 seconds, 72 degrees centigrade for 30 seconds, and 72 degrees centigrade for five minutes.

Following PCR amplification, 50 microliters of AMPure XP beads was added to each well, and the plate incubated at room temperature and on the magnetic stand for a total of 20 minutes. The supernatant was removed, and 200 microliters of 80% ethanol was used for two washes as described above. The wells were incubated on the magnetic stand for 15 minutes, and removed, upon which 32.5 microliters of Resuspension Buffer was added to each well of the plate. The plate was then incubated on the magnetic stand for five minutes, and 30 microliters of the supernatant was transferred to centrifuge tubes and stored for further downstream analysis.

2.4 RNA-Seq

RNA-seq was conducted utilizing an adapted protocol from Illumina. High-throughput sequencing was performed using a NextSeq500 sequencing system (Illumina) in the Genomic Resource Laboratory of the University of Massachusetts, Amherst. Complementary DNA libraries were single-end sequenced in 75 cycles using the NextSEquation 500 High Output Kit (FC-404-1005; Illumina) in a multiplex run of twenty discrete samples.

RNA-seq was conducted for n=3 samples per group (Control WT or Control KO) for the mTORC1 experiment and n=4 samples per group for the mTORC2 experiment. For mTORC1, the average number of reads was 38.8 million reads per sample, with the average percentage of reads aligned to the reference genome (mm10) being 90.2%. For mTORC2, the average number

of reads was 26.3 million reads per sample, with the average percentage of reads aligned to the reference genome (mm10) being 84.7%.

2.5 Western Immunoblotting

Western blotting was conducted using Thermo-Fischer Scientific Kit Numbers 78510 and 23225/23227 and an adapted protocol from Thermo-Fischer Scientific (Pub. No. MAN0011386). Unless otherwise indicated, all materials and kit numbers are from the above.

Protein was extracted using T-PER reagent with added protease inhibitor, in a ratio of approximately 100 mg liver tissue to 2 mL of prepared T-PER reagent. This mixture was homogenized at 10,000g until tissue was completely ruptured. The supernatant was collected and isolated into 100 microliter aliquots.

Sample quantification was completed following a standard curve preparation, using an albumin standard (BSA) for the curve preparation. The standard curve was prepared according to the manufacturer's instruction (Thermo-Fischer Scientific Kit 23225/23227).

Specimen was prepared in a solution of 4X Laemmili Buffer dye diluted 9:1 with 9 parts Laemmili Buffer and 1 part beta-mercaptoethanol. A standardized amount of protein was added, with buffer added in a ratio of 1 part buffer dye to 3 parts sample. This mixture was boiled for five minutes on a thermo-cycler and cooled on ice for five minutes.

Gel loading was done with Tris-glycine SDS as a running buffer, and the gel was run at 50V until migration out of the wells was observed, at which point the gel was run at 100V for approximately one hour.

Gel transfer was accomplished with the use of nitrocellulose membrane, with the membrane placed in transfer buffer for 10-15 minutes. The transfer buffer consisted of a mixture of 100 mL

methanol, 100 mL of running buffer, and 800 mL of deionized water. Transfer was done on ice with a running voltage of 15V for overnight.

Blocking was done with a solution of 3% blotting-grade skim milk for one hour at room temperature, and primary antibody targeting was completed in 3% blotting-grade skim milk overnight at 4 degrees centigrade. Secondary antibody incubation (Abcam Cat. No: ab6721) in a solution of 3% blotting-grade skim milk, was conducted following 5 rinses with 1X TBS-T buffer (100 mL 10X TBS, 900 mL deionized water, 2 mL of Tween-20), for 45-60 minutes. The blot was illuminated with Pierce ECL Western Blot Substrate (Thermo-Fisher Cat. No: 32106) and scanned with a Syngene G:BOX F3 scanner at the Department of Veterinary and Animal Sciences at the University of Massachusetts, Amherst.

2.6 Analysis of RNA-Seq data

To analyze the data from our mRNA sequencing experiment, read filtering, trimming, and de-multiplexing were performed via the BaseSpace cloud computing service supported by Illumina (available at: https://basespace.illumina.com/home/index). Furthermore, the preprocessed reads were mapped to the reference mouse genome (MM10) using the TopHat2 aligner (14). Aligned reads were then used for assembly of transcripts using Cufflinks, version 2.1.1, and differential expression of reference transcripts using Cuffdiff, version 2.1.1 (15). Differential expression data sets were further used for gene set enrichment analysis (GSEA, Broad Institute, Boston, MA; available at: www.broadinstitute.org/gsea).

Following completion of RNA-seq, bioinformatic analysis using Metascape, Gene Set Enrichment Analysis, and Ingenuity Pathway Analysis (IPA) was conducted (16, 17, 66). Metascape was conducted using default settings. RNA-seq data meeting a q-value of 0.05 or below was selected for further analysis. A list of genes found in the raw data for mTORC1 and mTORC2 KO that demonstrated statistical significance was taken and analyzed via Metascape. This list is hereafter referred to as the RNA-seq shortlist for both mTORC1 and mTORC2. Gene Set Enrichment Analysis was conducted using default settings (16), and cutoff values were assigned as a normalized enrichment score (NES) of >1.70 and a false discovery rate (FDR) value $q<0.1$. IPA was conducted using default settings, utilizing the aforementioned RNA-seq shortlist. Figures of canonical and disease pathways for knockout groups, as well as upstream and downstream analysis were generated through the use of IPA (QIAGEN Inc., https://www.qiagenbio- informatics.com/products/ingenuity-pathway-analysis).

GSEA was conducted using the Hallmark, C2, C3, and C5 collections of gene sets.

Hallmark is a collection of discrete gene sets computationally generated from the overlap of multiple “founder” gene sets for a particular biological process. The genes present in overlap are defined as having coherent expression, and are combined together to create a discrete Hallmark gene set (96).

C2 is a collection of gene sets that is curated from multiple sources, including online pathway databases and biomedical literature.

C3 is a collection of gene sets that represents targets of transcription factor or microRNA regulation, with each set containing genes that are grouped by short sequence motifs that are conserved in their non-protein coding regions.

C5 is a collection of gene sets that are derived from gene ontology annotations. The gene sets in this collection are based on specific gene ontology terms and belong to one of the three following categories: Molecular Function, Cellular Component, and Biological Process. Gene ontology terms that yielded very broad categories with very large gene sets were eliminated, as were terms that produced gene sets with fewer than five genes in total.

All gene collection sets that yielded results in line with the cutoff values described above are discussed in the results section.

Following GSEA analysis, a comparison of mTORC1 KO and mTORC2 KO data sets revealed a subset of genes that were changed both in mTORC1 KO and mTORC2 KO animals. These genes were additionally visualized using Metascape.

In the next step of our analysis, we used the aforementioned collection of genes that were differentially expressed in both mTORC1 KO and mTORC2 KO animals for a functional analysis. These genes were identified from the raw data for statistically significant (FDR q value

<0.05) gene expression changes, and genes that appeared in both the mTORC1 KO list and the mTORC2 KO list were included as differentially expressed for both mTORC1 and mTORC2.

We used IPA in order to visualize the activity of upstream regulators that were most likely leading to the changes in gene expression that we saw in our RNA-seq shortlist data. Following this analysis, we were able to construct a map of mTORC1 and mTORC2 signaling through these regulators, and were able to visualize what the predicted states of these regulators would be in a knockout genotype of either complex. We then utilized STRING (84) in order to illustrate protein-protein interactions amongst the regulators that were found in our IPA upstream analysis results. Following this, any upstream regulator that did not have a known interaction with other regulators in the list was selected for a literature review in PubMed. This was conducted separately for mTORC1 and mTORC2 upstream regulators, using the key words “regulator name” and “liver” or “hepatocellular carcinoma” or “mTOR” or “mTORC1” or “mTORC2” or “function.”

CHAPTER 3

RESULTS

3.1 Confirmation of mTORC1 and mTORC2 KO: RNA-seq results and western immunoblot of mTORC1 and mTORC2 liver samples

To confirm that our knockout model succeeded, we performed western immunoblotting for mTORC1 and mTORC2 wild-type and KO liver cell lysates. We additionally analyzed our RNA-seq data for the direction of expression change in Raptor and Rictor, respectively. As was expected, knockout of Rictor in mTORC2 experiment mice yielded complete absence of phosphorylated AKT, a target of mTORC2 signaling (**Figure B.5)**. mTORC1 results similarly showed severely reduced amounts of phosphorylated p70S6K, a target of mTORC1, as compared to control. However, there remained a small amount of phosphorylated pP70S6K in the blot, indicating that Raptor knockout almost completely abrogated phosphorylation of p70S6K, but did not fully abolish it (**Figure B.5)**. In addition, we found that both Raptor and Rictor were downregulated in our RNA-seq shortlist data, as shown in **Figure B.5.** These results are further elaborated upon in the discussion portion of this manuscript.

3.2 Genes Differentially Expressed in the mTORC1 KO Experiment:

For mTORC1, **Figure B.1** shows significant enrichment for multiple gene functional groups, with the highest enrichment shown for steroid metabolic process, response to stilbenoid, monocarboxylic acid metabolic process, and mitotic cell cycle. The –Log10(P) value indicates the likelihood that a shown enrichment is due to chance, with a more negative value indicating that the enrichment is very unlikely due to chance alone (18). mTORC1 is known to play a main role in growth signaling regulation, cell division activity, and nutrient abundance (1), so the knockout of this complex would explain enrichment in genes involved in these same processes.

Figure B.1 additionally shows that regulation of wound healing and responses to chemokines are enriched, both which are functions of the innate immune system (55). With a significant amount of mTORC1 focused research and review describing immune-mediated effects (56, 57), we did not find it unexpected to note immune-related gene enrichments following a perturbation of mTORC1 function.

It is important to note that the enrichment found in Metascape analysis does not indicate direction of gene expression change, that is, it is not possible to say from Metascape visualization alone if gene expression is being up or downregulated. Therefore, further downstream analysis was conducted for both complexes in order to better understand gene expression changes.

3.3 Genes Differentially Expressed in the mTORC2 Experiment

For mTORC2, **Figure B.2** shows significant enrichment for genes involved in the monocarboxylic acid metabolic process, the monocarboxylic acid biosynthetic process, regulation of small molecule metabolic process, and triglyceride metabolic process. With mTORC2 known to be an activator of Akt1, as well as PKC and SGK (4), effects on metabolic processes and synthesis of triglycerides, both important for cellular activity as well as for core cellular functions (58), is an expected finding in an mTORC2 knockout genotype.

Surprisingly, we noted enrichments in genes responsible for monocyte differentiation, cell chemotaxis, neutrophil degranulation, and positive regulation of NIK/NF-kappaB signaling. These functions are all well-known responses that define both an innate and an adaptive immune response (60). However, most research to date has implicated mTORC1 as a known activator of NFkB signaling (59), so an observed enrichment of these mTORC1-implicated functions in an mTORC2 knockout genotype was an unexpected result. Chemokine enrichment was also observed in **Figure B.1,** following mTORC1 perturbation, with chemokines functioning as cell attractants in innate as well as in adaptive responses (55, 60). Neutrophil degranulation is well-conserved, innate immune system mediated regulator of cytotoxicity (60), and its observed enrichment following mTORC2 knockout was an additional interesting observation.

As for mTORC1 knockout, Metascape analysis only shows enrichment and does not indicate upregulation or downregulation of gene expression. Therefore, the immune-related results above do not point to positive or negative regulation of the respective immune functions, but indicate that changes in these functions occur in mTORC2 knockout animals. These results, along with mTORC1 knockout results, are explored further in the following sections.

3.4 RNA-seq data yields a list of commonly enriched genes in both groups

There were a small number of genes that were either not specifically referenced in the literature, did not exist in humans, or did not have any known function/literature related to their roles in hepatocellular carcinoma (HCC), liver/hepatocyte function, or NAFLD. These genes were *Lect1 and Clec2h. Lect1* did not have any articles related to liver, HCC, or NAFLD. *Clec2h,* while shown to be upregulated in male and female offspring of mice fed a Western high cholesterol, high fat diet (19), has no human ortholog, and these two genes were not pursued further due to lack of translational relevance. The total number of translationally relevant genes identified, therefore, was 21, as summarized in **Table A.1**. A comparison of the total number of genes changed in mTORC1 KO and mTORC2 KO, along with the aforementioned commonly changed genes, is shown in a **Figure B.4.**

A summary of the known functions of the protein product of each of the 21 genes found to be changed in mTORC1 and mTORC2 KO mice was adapted from the NCBI (National Center for Biotechnology Information) database, and is shown **Table A.1**.

Following the determination of a list of 21 genes found to be perturbed in both mTORC1 KO and mTORC2 KO experimental groups, a search in PubMed was conducted using the key words: 'gene x' or 'gene x and liver' or gene x and hepatocellular carcinoma' or 'gene x and Non-Alcoholic Fatty Liver Disease (NAFLD).' The identifier *gene x* refers to any of the 20 genes, as this search was conducted identically for all genes in the list. No limit was placed on the year of publication, and no language limits were applied.

Following the identification of the 21 genes found to be perturbed in both mTORC1 KO and mTORC2 KO experimental groups, results in the literature were separated into three groups as follows: hepatocellular carcinoma/liver cancer, NAFLD or fatty liver, and related

diseases/human morbidities. These three groups are presented in **Table A.1.** A detailed annotation of each gene is presented in Appendix C of this manuscript.

3.5 An analysis of genes affected in both KO groups

For the shortlist of genes responding to both mTORC1 and mTORC2 KO, Metascape analysis showed strong enrichment of genes involved in the monocarboxylic acid metabolic process, as well as in other lipid metabolic processes (Figure **1.c**)

An overview of the 23 genes found to be responding both to mTORC1 and mTORC2 KO was created as described in the methods section. This is found in **Figure B.3**. Interestingly, the results show similar enrichment that was found in mTORC1 and mTORC2 knockout groups using Metascape analysis, as visualized in **Figures B.1 and B.2.** These results, in addition to the gene set enrichment analysis results, are discussed at length in the discussion portion of this manuscript.

3.6 Gene Set Enrichment for mTORC1 and mTORC2 KO groups

3.6.1 mTORC1

GSEA results that met our cutoff values included the Hallmark collection of gene sets, C2 collection of gene sets, and the C5 collection of gene sets.

Hallmark results showed a negative enrichment for genes involved in Bile Acid metabolism, as well as in xenobiotic metabolism and cholesterol homeostasis. Positive enrichment was shown for genes involved in E2F and G2M targeting, as well as in allograft rejection and immune-inflammatory signaling. These are visualized in **Table A.2.**

Upon a further exploration of both bile acid metabolism as well as cholesterol homeostasis, we found that the activity of both of these processes is linked, with bile acid signaling via G-Protein coupled receptors critical for regulating hepatic glucose and lipid homeostasis, and

cholesterol catabolism to bile a key component of tight cholesterol homeostasis (60). Notably, the activity of both of these processes is known to be regulated in an enterohepatic circuit, with Akt/mTOR activity a key regulator of the aforementioned circuit (60).

E2F and G2M targeting both refer to cell cycle checkpoint targeting, with mTORC1 activation known to be a positive regulation of cell division and cell growth (1). However, our results noted strong positive enrichment targeting of the cell cycle, indicating that mTORC1 knockout promoted cell cycle progression, the opposite of what would be expected. Notably, allograft rejection and immune-inflammatory signaling were positively enriched in mTORC1 knockout mouse hepatocytes, an unusual result as well given the known roles of mTORC1 both in tissue rejection as well as in immune related inflammation (1,62,63).

C2 collection results showed a negative enrichment for Reactome and Kegg (Kyoto Encyclopedia of Genes and Genomes) pathways involved in cholesterol biosynthesis as well as in gene expression activation via Srebf. Positive enrichment was shown for Reactome pathways involved in translational and transcriptional activity, as well as in rRNA processing, cell division activity, and response to influenza infection. These are visualized in **Table A.3.**

As was observed for **Table A.2,** positive enrichments were for cellular processes that are regulated by mTORC1, an unexpected finding given that mTORC1 knockout should have theoretically suppressed these categories. Subsequent gene ontology analysis using the C5 collection of gene sets, visualized in **Table A.4,** showed positive enrichment for genes functioning in ribosomal synthesis and bioactivity, as well as in genes functioning in cell division, protein localization, and regulation of lymphocyte migration. As was observed in **Tables A.2 and A.3,** the knockout of mTORC1 yielded an unexpected positive enrichment for functions that were predicted to be negatively affected by mTORC1 perturbation.

3.6.2 mTORC2

C2 results showed positive enrichment for Reactome pathways involved in ribosomal activity, rRNA processing and activity, as well as in DNA processing activity. Interestingly, positive enrichment was observed for response to influenza infection, as was shown in **Table 2.a** for mTORC1 KO. Additional similarity in results to mTORC1 was displayed for rRNA processing, nonsense-mediated decay, and selenoamino acid metabolism. All of the C2 mTORC2 KO results are detailed in **Table A.5.**

C5 results showed positive enrichment for genes functioning in ribosomal activity and protein localization. These overlapped with C5 results for mTORC1, with the highest enrichment values for the C5 collection being cytosolic ribosome gene ontologies for both mTORC1 and mTORC2 groups. These results are detailed in **Table A.4** for mTORC1 and **Table A.6** for mTORC2.

3.7 Common Enrichments in mTORC1 and mTORC2 KO groups

GSEA results yielded a set of enrichments terms that were positively enriched both in mTORC1 KO and mTORC2 KO mice. These results are detailed in **Table A.7.** Interestingly, positive enrichment was observed for KEGG pathways, Reactomes, and Gene Ontologies that would have been expected to have a negative enrichment upon mTORC1 or mTORC2 knockout. Following this observation, we conducted follow-up work to uncover both the identities of genes that are changed in both mTORC1 and mTORC2 KO animals.

To add to the observations in **Table A.7,** we compiled a datasheet (data not shown) in order to gain an understanding of the identities of each gene changed in the enriched categories in **Table A.7**. The results in this dataset show that almost all of the genes enriched in both mTORC1 and mTORC2 KO animals are genes belonging to the ribosomal large and small subunits. Indeed, these results are consistent even in categories that initially may not appear to be centered on

ribosomal activity, such as Reactome_Influenza_Infection and Reactome_Selenoaminoacid_Metabolism.

3.8 Ingenuity Pathway Analysis of mTORC1 and mTORC2 KO Groups

3.8.1 mTORC1 KO results

In order to completely describe mTORC1 signaling, we first visualized impacts of mTORC1 KO in respect to core cellular functions and to common disease states of an organism. As visualized in **Figure B.6,** strong negative enrichments are observed in pathways responsible for the synthesis of cholesterol, as well as for activation of LXR/RXR and FXR/RXR, the former known to regulate cholesterol biosynthesis as well. The only positively enriched category out of the top 15 enriched categories was the Sirtuin signaling pathway, an interesting finding whose translational aspects is elaborated upon in the discussion portion of this manuscript.

In regards to the top 15 disease categories enriched in mTORC1 KO animals, the highest enrichments were observed for lipid metabolism, small molecule biochemistry, and vitamin and mineral metabolism, as shown in **Figure B.7.** Additional enrichments were observed for metabolic disease, organismal injury and abnormalities, cell death and survival, and endocrine and gastrointestinal disease. All enrichments were well above the threshold value, as shown by a p-value of less than 0.05.

3.8.2 mTORC2 KO results

In contrast to mTORC1 KO data, mTORC2 KO showed significant enrichments in the top 15 categories of cellular canonical pathways, but did not show direction of enrichment, as shown in **Figure B.8.** Indeed, two of the top 15 canonical pathways shown did not have any activity data available. This may be a result of the limited research on mTORC2 as compared to mTORC1,

leading to the mTORC2 associated pathways not being as well studied or even identified, as are associated pathways.

For disease pathways enriched with mTORC2 KO, lipid metabolism was a top enrichment, as it was for mTORC1 KO. Additional similarities were observed in small molecule biochemistry enrichment as well as in organismal injury and abnormalities and gastrointestinal disease. Unique categories were for hepatic system disease as well as for metabolic disease, with all enrichments detailed in **Figure B.9.** P-values were similarly well below threshold as they were for the mTORC1 KO data, indicating statistical significance of findings.

3.9 mTOR Upstream Regulator analysis

3.9.1 mTORC1 KO Results

Following the general findings afforded to us by the canonical and disease pathway analysis, we utilized the same shortlist from mTORC1 KO RNA-seq data in order to describe the regulators of the genes that were altered in the shortlist data. These results were sorted based on the type of upstream regulator, with our analysis focusing on transcription regulators and ligand-dependent nuclear receptors. This analysis included the predicted activation score; a calculated value based on the activation z score, which was calculated from the activation states of the target molecules found in our RNA-seq shortlist dataset. In the knockout genotype, upstream regulators that were predicted to be inhibited included PPARA, SREBF1 and SREBF2, as well as other upstream molecules such as TRIM24, HOXA10, MAF, and STAT5B.

In the same dataset, upstream regulators that were activated included RARA, CREB1, E2F3, NFKB2, and JUN, among others. These results are summarized in **Figure B.10,** and the roles of these various factors are all described in the discussion section of this manuscript.

3.9.2 mTORC2 KO results

For mTORC2 KO data, an identical protocol was followed for generation of the list of upstream regulators as for mTORC1 KO. In this dataset, there were no positive upstream regulators that met a p-value of 0.05 or lower, and there were overall significantly fewer upstream regulators found that met statistical significance than were found for mTORC1 KO data. However, there was one upstream regulator, STAT5B that was predicted to be negatively activated in this data set as well as in the mTORC1 KO data set. This is shown in **Figure B.11.** Additional upstream regulators that were predicted to be negatively regulated included PPARD, RORA, and MLX, among others. The roles of these factors are all described in the discussion section of this manuscript.

3.10 STRING Analysis for Upstream Regulator results

3.10.1 mTORC1 results

mTORC1 STRING analysis generated a total of three upstream regulators that had no predicted interaction with one another and/or with any of the remaining upstream regulators. As visualized in **Figure B.12,** these three were Sirt2, Hoxa10, and Kdm5b. The role of each gene was determined via a literature search in PubMed, and the results and implications are elaborated upon at length in the discussion portion of this manuscript.

3.10.2 mTORC2 results

mTORC2 String analysis generated a total of five upstream regulators that had no predicted interaction with one another and/or with any of the remaining upstream regulators. As visualized in **Figure B.13,** these five were Etv5, Rora, Ppard, Mlx, and Zbtb20. The role of each gene was determined via a literature search in PubMed, and the results and implications are elaborated at length in the discussion portion of this manuscript.

3.11 mTOR Downstream Signaling Analysis

3.11.1 mTORC1 KO results

Following the determination of the activity of genes that are known regulators of our mTORC1 KO shortlist genes, we constructed a signaling pathway based on these data, with mTORC1 at the center, in order to show how each regulator interacts with each other, and the role of mTORC1 in the signaling mediated through these different regulators. This pathway is shown in **B.14,** with red indicating negatively regulated, and green indicating positively regulated. As is visible in the pathway, mTORC1 KO promotes the activation of SREBF2, the inhibition of CREB, and the inhibition of activated SREBF1. From these three molecules, downstream effectors are either activated or inhibited. These effects are most likely responsible for the activation states of the genes in our mTORC1 KO RNA-seq shortlist.

3.11.2 mTORC2 KO results

In the same manner as was done for mTORC1 data, we constructed a signaling pathway, with mTORC2 at the center, in order to demonstrate how each regulator interacts with each other. This pathway is shown in **Figure B.15,** with white indicating an indirect connection between the two genes, and green indicating positive regulation. Importantly, there is an *indirect* connection between mTORC2 and SREBF1, through which the remaining downstream entities, shown in green, are activated. This indirect relationship is likely due to the overall lack of knowledge data of mTORC2 downstream targets as compared to mTORC1.

CHAPTER 4

DISCUSSION

4.1 Overview

Much research has been devoted to the elucidation of mTOR signaling, with a majority of research focusing on the role of mTORC1 due to its aforementioned modulation by the immunosuppressant drug rapamycin. However, the role of mTORC2 is not as well described and the role of mTORC1 and mTORC2 in concert has yet to be elucidated. As mentioned in previous sections, the most recent research from Lamming et.al and Gruppuso et.al have not used a model with a liver specific knockout of mTORC1 *and* mTORC2 from gestation. We have also not seen a complete bioinformatic analysis of transcriptome product from these aforementioned liver-specific knockout mice, and as such noted the existence of incompleteness in the scientific literature in respect to liver-specific mTOR signaling describing both mTORC1 and mTORC2.

In order to describe mTOR signaling in the manner set forth in the above section, we utilized the latest developments in next-generation bioinformatic analysis in order to achieve our results. Through the use of RNA-seq followed by analysis with Metascape, GSEA, and IPA, we have been able to describe mTOR signaling in the liver with a level of depth that has been lacking in the current literature. Our discussion of our results is presented in the following sections.

4.2 mTORC1 and mTORC2 KO yields a list of commonly altered genes

As shown in **Table A.1**, our initial RNA-seq data yielded a list of genes that were altered in both mTORC1 KO and mTORC2 KO groups. Furthermore, we found that all 21 of these genes that were found to have translational relevance had a known role in NAFLD, HCC, or a related human morbidity. These results are significant due to the common usage of rapamycin and its related rapalogs for immunosuppressive purposes. The changes in these genes and their role in human disease indicates that certain side effects of rapamycin treatment may extend to changes in transcription of genes that are unrelated to the therapeutic use of the drug. This information will likely prove vital to further translational study of the long-term effects of rapamycin treatment by providing particular markers of transcriptional change. Additionally, since these genes were changed in perturbation of both mTORC1 and mTORC2, there is now additional evidence that both complexes regulate multiple different genes. This is important for the understanding of how complex diseases such as hepatocellular carcinoma and non-alcoholic fatty liver disease progress, and provides a more detailed overview of the signaling that may be responsible for disease progression.

4.3 Bioinformatic analysis of mTORC1 and mTORC2 KO data

Our work has shown that the knockout of mTORC1 and mTORC2, respectively, leads to both expected and unexpected changes in the mouse liver transcriptome. In addition, we found that there were changes in genes responsible for ribosomal biogenesis upon knockout of mTORC1 and mTORC2, indicating that signaling from both mTOR complexes is likely responsible for ribosomal biogenesis.

Interestingly, results from Metascape analysis of mTORC2 KO data showed that there were enrichments in immune system-related functions, which has until now been known to be

regulated by mTORC1 signaling. As shown in **Figure B.1**, these changes were an unexpected finding due to their known association with mTORC1 signaling. Since the ubiquitous mTORC1 inhibitor rapamycin is used as an immunosuppressant, the regulation of certain immune system functions by mTORC2, as suggested by our data, may help explain cases of resistance to rapamycin therapy, and may open the field to research on mTORC2 inhibition for particular immune system disorders.

Further analysis with GSEA revealed additional unexpected findings of mTOR signaling perturbation. As shown in **Table A.2**, mTORC1 KO leads to an upregulation of gene sets known to function in cell division as well as in allograft rejection and innate immune response activity. These results were the opposite of what was expected. Given that mTORC1 is known to regulate these same functions, we expected a knockout of this complex to lead to a downregulation of these functions. These data provide a view of mTORC1 signaling that has not been previously described, and these findings suggest that there are likely other signaling complexes that regulate mTORC1-dependent functions.

In addition, we have found that there is a subset of gene ontology results for mTORC1 KO and mTORC2 KO that are similarly enriched, with positive upregulation of gene ontologies that would have been expected to be negatively regulated upon mTORC1 or mTORC2 knockout. These results, as detailed in **Table A.7**, show common enrichments of gene ontologies for both knockout genotypes, with a positive enrichment shown for all. These results indicate that in knockout of either complex, ribosomal biogenesis, DNA repair, and certain immune functions are all enriched. Given that the current research suggests that mTOR signaling controls these processes, we expected that a knockout would have suppressed these functions.

A more detailed look reveals that the individual genes that compose each enrichment ID category were ribosomal protein genes. Therefore, even categories such as Reactome_Influenza_Infection and Reactome_Selenoamino_Acid_Metabolism were all composed of ribosomal proteins. Ribosomes were likely formed during the period of humanity's Last Common Universal Ancestor (LUCA), and they are necessary for translating all mRNA into protein (85-87). Therefore, ribosomes are critical for sustaining life itself, as protein products function in heterogeneous roles spanning development, cell division, cell death, cell differentiation, defense and immunity, and cell signaling. Signaling from mTORC1 is known to regulate aspects of cell division, and mTORC2 signaling is known to regulate cell proliferation (1), with ribosomes being key for protein translation that regulates these processes. Therefore, an increased enrichment in ribosomal proteins in response to both mTORC1 and mTORC2 knockout likely indicates that there are compensatory mechanisms in place that maintain key cell functions even in the absence of mTOR signaling.

Additional support for our findings comes from Western immunoblots, shown in **Figure B.5.** We found that upon knockout of Raptor, the phosphorylation of p70S6K was significantly reduced to almost non-existent levels, while a corresponding rise was seen in the amount of phosphorylated AKT, a known target of mTORC2 signaling. This type of compensatory response was seen in the mTORC2 experiment group as well, with a knockout of Raptor leading to abrogated phosphorylation of AKT, while yielding a smaller, but still noticeable increase in phosphorylated p70S6K as compared to controls. This gives further credence to our observation that abrogation of one complex's activity brings about increased signaling through the other. We have yet to see any mention in the literature of a compensatory increase in liver-specific mTORC1 or mTORC2 signaling following the knockout of one of the two complexes, and our

results show that there is likely cross-talk between mTORC1 and mTORC2. This finding may have translational relevance as well, as rapamycin, an mTORC1 inhibitor, is frequently used as an immunosuppressant following organ transplantation as well as in exploratory uses against certain forms of cancer. Understanding that the targeted silencing of one mTOR complex may bring about increased signaling of the other complex is critical for explaining off-target drug effects, cellular proliferation, and other related changes that may occur. While it is currently unknown specifically what effects arise following an upregulation of one mTOR complex following the inhibition of the other, further studies are needed to explore this unique, liver-specific mTOR signaling relationship.

4.4 IPA analysis reveals potential translational implications of liver-specific mTOR inhibition

Two very significant causes of human morbidity and mortality are non-alcoholic fatty liver disease, also known as non-alcoholic hepatosteatosis, and hepatocellular carcinoma (HCC) (67-71). For HCC, treatment options and prognosis for non-resectable disease consist of hepatic arterial infusion chemotherapy, radiation therapy, and the multi-kinase inhibitor sorafenib (73, 74). However, overall survival for metastatic, non-resectable HCC was increased to only 10.7 months with sorafenib treatment as compared to 7.9 months with placebo (73). While there has been a recent clinical trial that has described some benefit of administration of the multi-kinase inhibitor regorafenib following sorafenib therapy (75), clinical outcomes for advanced HCC remain poor.

Recent research has suggested that the sirtuin signaling pathway may mediate poor outcomes of sorafenib therapy, specifically via the SIRT1 deacetylase, a key human sirtuin (76). A previous study has noted that overexpression of SIRT1 is associated with a poor response in

HCC (77). The role of SIRT1 in HCC is not completely understood, however, research suggests that SIRT1 plays a role in HCC progression by regulating the activity of other key oncogenic proteins, thereby promoting cancer progression (77). Therefore, SIRT1 may be a significant biomarker of HCC progression, and remains an important research target towards sorafenib-resistant HCC.

Our IPA results have shown that the sirtuin-signaling pathway is significantly upregulated in mTORC1 KO mice (**Figure B.6)**. The most recent research on SIRT1 and HCC has shown downregulation of mTORC1 phosphorylation following treatment of HCC cell lines with sorafenib, indicating that sorafenib has an inhibitory effect on mTORC1 in HCC (76). Since SIRT1 is implicated in sorafenib resistance in advanced HCC, it is interesting that mTORC1 inhibition was induced by sorafenib treatment in this research, particularly because our work has shown sitruin signaling enrichment following mTORC1 knockout. This may explain the eventual decline of patients treated with sorafenib, possibly occurring via a sorafenib-induced downregulation of mTORC1. Following this downregulation, there may be an associated increase in sitruin signaling that we observed in our results. This may then mediate increased SIRT1 transcription and activity, and the subsequent resistance to sorafenib treatment. While these research findings are preliminary, they suggest an important link between mTORC1, the sitruin signaling pathway, and sorafenib resistance in advanced HCC. More research would be needed in order to further elucidate the mechanisms of resistance, as well as possible secondary targets for sorafenib-resistant HCC.

4.5 IPA reveals a subset of novel downstream effectors of mTORC1 and mTORC2 signaling

4.5.1 mTORC1 results

IPA analysis allowed for a clearer picture of mTORC1 signaling in mouse hepatocytes, and additionally allowed for the use of STRING to test for interactions between individual upstream regulators. As shown in **Figure B.12**, three upstream regulators in total did not have any predicted connections between themselves and other upstream regulators. Following further research, we discovered that there was very little in the primary literature that related mTORC1 signaling to these three genes, indicating a likely novel relationship and an unexplored area of mTORC1 signaling in the liver

A literature search for Sirt2, a protein from the family of NAD-dependent deacetylases, revealed heterogeneous activity in the liver. Sirt2 has been discovered to facilitate liver glucose uptake, and its overexpression enabled metabolically obese mice to overcome their glucose intolerance via increased glucose uptake. A knockdown in non-diabetic mice induced glucose intolerance and decreased hepatic glucose uptake (88). Our results indicated inhibition of Sirt2 in an mTORC1 KO genotype, indicating a potential of hepatic glucose intolerance in patients treated with rapamycin or rapalogs due to their suppression of mTORC1 activity. However, Sirt2 overexpression was found to be a predictor of poor survival and increased metastatic events in patients with HCC (89), as well as a promoter of increased hepatic fibrosis (90), indicating that while mTORC1 suppression may lead to specific off target effects, some of these effects may not be clinically detrimental.

Kdm5b, a type of lysine-specific demethylase, also lacked any known connection to mTORC1, with its most notable association being a prognostic factor for hepatocellular

carcinoma, in which increased Kdm5b expression was found to promote tumor cell progression and was associated with a poor prognosis in clinical samples (91). Our results indicated that mTORC1 knockout inhibited Kdm5b, indicating a possibility for the use of mTORC1 inhibitors in Kdm5b-driven HCC.

Hoxa10, part of a family of homeobox transcription factors, was another potential clinical target, with a recent study pointing to its knockdown as suppressive in an *in vitro* and an *in vivo* model of HCC (92). As was the case for Kdm5b, we noted an inhibition of Hoxa10 in mTORC1 KO IPA results, indicating that Hoxa10, along with Kdm5b, could be a possible clinical target for HCC treatment.

While any translational relevance from the above results is clearly preliminary, a noted discovery is the association of mTORC1 with these three proteins, all of which play a role in significant human morbidity and mortality. Further research should be aimed at elucidating the mechanisms by which mTORC1 signaling mediates changes in the expression of these three genes. Additional attention should also focus on the effects of mTORC1 inhibition in treatment of advanced HCC driven by these genes, from which significant clinical benefit may result.

4.5.2 mTORC2 Results

IPA results of upstream regulator analysis for mTORC2 KO RNA-seq shortlist data yielded five total genes that did not have any known association with the other upstream regulators identified, with results shown from STRING analysis in **Figure B.13.** A literature review yielded potential translational implications for mTORC2 inhibition in the context of these five genes, all of which were predicted to be inhibited in an mTORC2 KO genotype.

With respect to liver lipid balance, two of the five genes noted in IPA results have a defined role in liver lipid homeostasis. The zinc finger protein Zbtb20 is known to promote *de-novo* hepatic lipid synthesis (93), and its absence is defined by hypolipidemia and impaired lipid synthesis in mouse hepatocytes. The retinoic acid receptor-related orphan receptor RORα also controls liver lipid homeostasis through its interactions with PPARγ, with mice lacking RORα developing steatohepatitis, obesity, and diabetes (94). Interestingly, Zbtb20 downregulation as predicted by our IPA results would lead to hypolipidemia, the opposite of which would likely occur in RORα downregulation. While the clinical significance of these two divergent effects following mTORC2 KO requires significant further study, our results give evidence that a novel relationship exists between mTORC2 signaling and these two proteins, thus adding to the understanding of the mechanisms relating liver lipid balance and mTOR signaling.

MLX was a unique finding in our IPA analysis, as it functions as a transcription factor only after heterodimerizing with ChREBP. Together, MLX-ChREBP act as a response element to glucose, with a key function of this heterodimer being the upregulation of fatty acid synthase transcription following increased glucose levels in the liver (95). Mice with a disruption in ChREBP or a dominant negative form of MLX do not have induction of liver lipogenesis following carbohydrate stimulation (95). Our results indicate that MLX is inhibited in an

mTORC2 KO genotype, pointing to both a novel mTORC2-mediated regulation of lipogenesis control in the liver, as well as a potential mechanism by which excessive lipogenesis may be targeted.

Etv5 was the least studied of all genes that we discovered during our analysis, with no research found in PubMed relating its activity to the liver, mTORC2, or mTOR signaling in general. However, our results indicate that there is a relationship between mTORC2 knockout and Etv5 inhibition, and that this does not appear to proceed through any of the other upstream regulators found during IPA. Therefore, further research should be completed, perhaps by the generation of liver-specific knockouts of Etv5 in order to determine its role, if any, in liver function.

PPARδ is additionally under researched both in respect to its function in the liver as well as its association with mTOR signaling. As was noted for Etv5, more mechanistic research is needed in order to elucidate the specific role that this gene plays in the liver, especially given that our current results point to a relationship between mTORC2 inhibition and PPARδ inhibition.

4.6 IPA allows for a complete picture of mTOR signaling in both wild-type and knockout genotypes

Next-generation analysis using IPA allows for the construction of signaling pathways in ways that were not previously possible. In conjunction with upstream analysis, we generated a signaling pathway with either mTORC1 or mTORC2 in the center, as visualized in **Figures B.14 and B.15,** respectively. As our results from upstream analysis showed the predicted activation states in the case of an mTORC1 or mTORC2 knockout phenotype, we wanted to determine what a wild-type signaling pathway would conceivably look like in hepatocytes.

Our results indicate that mTORC1 and mTORC2 signaling initiates with some similarities, as both mTORC1 and mTORC2 signaling initiates through SREBF1. However, similarity ends at that point, with mTORC1 signaling additionally activating SREBF2 and deactivating CREB, leading to a unique mTORC1-specific downstream signaling response, visualized in **Figure B.14.** mTORC2 (**Figure B.15)**, on the other hand, brings about downstream signaling via activation of entirely different transcription factors, and notably differs from mTORC1 signaling in that all downstream effectors are activated.

In combination with our discovery that there are multiple unique transcription factors functioning in hepatic mTORC1 and mTORC2 signaling, we have uncovered significant evidence that hepatic mTORC1 and mTORC2 signaling is divergent, and has multiple currently uncharacterized downstream proteins associated with its signaling. This is important both in understanding the basic mechanisms of hepatic mTOR signaling as well as in elucidating why responses to rapamycin and its associated rapalogs may be incomplete or ineffective at treating certain hepatic malignancies. While our data does not directly implicate one of the many downstream effectors perturbed in hepatic mTORC1 and mTORC2 knockout animals in the progression of HCC, it suggests that there are multiple possible targets that require further study.

CHAPTER 5

CONCLUSION

mTORC1 and mTORC2 signaling in hepatocytes has been an area of recent interest, culminating with significant works by Lamming et.al and Boylan et.al that profiled the activity of mTOR signaling in mouse as well as Sprague-Dawley rat hepatocytes. However, the models used were not directly comparable to one another due to the differing ways that mTORC1 and mTORC2 were inhibited, and microarray analysis did not achieve whole genome analysis of mTORC1 and mTORC2 perturbations.

In our approach, we used a liver-specific knockout of mTORC1 or mTORC2, and performed RNA-seq and subsequent analysis using Metascape, GSEA, IPA, and STRING in order to thoroughly characterize the activity of mTORC1 and mTORC2 in the mouse hepatocyte. Our results have shown that there are specific genes that are perturbed following either mTORC1 or mTORC2 knockout, and that the enriched genes have a role in HCC, NAFLD, or a related human morbidity. Subsequently, we found common positive enrichments for ribosomal biogenesis, DNA repair, and certain immune functions, allowing for us to conclude a common role of both signaling complexes in these critical cell functions. Further analysis revealed that these enriched categories were composed almost entirely of ribosomal genes, indicating that while both complexes likely regulate these genes, there must be alternative pathways in the hepatocyte that are activated following mTOR perturbation. Results of IPA and STRING revealed multiple downstream targets of mTORC1 and mTORC2 in the mouse hepatocyte that have not been described in the literature, thus adding to basic understanding of mTOR signaling in the liver. These novel downstream targets were also closely associated with HCC and lipid homeostasis in the liver, indicating that altered mTOR signaling may be responsible for

pathological changes in hepatocytes. While these results do not yet elucidate a single target for HCC or liver lipid homeostasis in relation to mTOR signaling, the relatively low number of novel downstream effectors identified yields a narrow list of potential clinical targets. Our findings also allow for the generation of liver specific mTOR signaling pathways, which include the aforementioned novel downstream targets, thus adding to basic mechanistic knowledge of mTOR signaling in the liver.

In conclusion, we have made significant progress in elucidating the details of mTOR signaling in mouse hepatocytes. Our models have allowed for clean comparisons between mTORC1 and mTORC2 knockout hepatocytes, and have given detailed information of possible clinical targets for the treatment of HCC or lipid homeostatic disruption. More research is needed in order to fully elucidate the role of novel downstream targets of mTOR signaling in the liver, and our data yields a starting point for these future pursuits.

APPENDIX A
TABLES

A.1 List of genes differentially expressed in both mTORC1 and mTORC2 knockout groups

Gene ID	Known Function Via NCBI	Hepatocellular Carcinoma	Non-Alcoholic Fatty Liver Disease	Other Human Morbidities
Rgs16 (Regulator of g-protein signaling 16)	Inhibits signal transduction by increasing the GTPase activity of G protein alpha subunits	-----	33	-----
Fasn (Fatty Acid Synthase)	Multifunctional protein whose main function is to catalyze palmitate synthesis from acetyl CoA and malonyl CoA. This palmitate is then catalyzed into long-chain fatty acids for storage	20	-----	-----
Acot1	Acyl-CoA thioesterase 1	-----	34	-----
Acot2	Acyl-CoA thioesterase 2	-----	35	-----
Serpina12	Known as Vaspin in literature	-----	36	-----
Myc (proto-oncogene myc)	Encodes a nuclear phosphoprotein that plays a role in cell cycle progression and in apoptosis as well as cell cycle progression	21	-----	-----
Adgrf1	Adhesion G-protein coupled receptor F1	-----	-----	39
Gna14	G protein subunit alpha 14 Guanine-nucleotide binding protein that may play a role in pertussis-toxin resistant activation of phospholipase C-beta and its related downstream effectors	22	-----	-----
Cyp26a1	Cytochrome p450 family 26 subfamily A member 1 Endoplasmic reticulum protein that acts on retinoids, including all-*trans*-retinoic acid, and regulates the levels of retinoic acids in the cell	23	-----	-----
Lepr	Leptin receptor, involved in the regulation of fat metabolism as well as in a novel hematopoietic pathway that is necessary for normal lymphopoiesis	32	-----	-----
Extl1	Exostosin-like glycosyltransferase Functions in the chain polymerization of heparan sulfate and heparin	24	-----	-----
Cd36	Liver lipid transport gene expressed in the liver that functions to transport lipids from the blood into liver fat stores	25	37	-----
Saa2	Serum amyloid A2 coding gene in humans and mus. Musculus Biased expression in liver, fat, and in lesser amounts in appendix	26-28	-----	-----
Dpy19l3	Dpy-19 like c-mannosyltransferase 3	-----	-----	41, 42
Mid1ip1	MID1 interacting protein 1	-----	38	-----
Agpat9	Lysophosphatidylcholine acetyltransferase 1, also known as Agpat9 Plays a role in lipid metabolism, specifically in the conversion of lysophosphatidylcholine to phosphatidylcholine in the presence of Acetyl-CoA	-----	-----	44, 45
Chpf2	Chondroitin polymerizing factor 2	-----	-----	40
Mir671	microRNA 671	29	-----	-----
Gpc1	Glypican 1 Cell surface heparan sulfate proteoglycan, may play a role in control of cell division and growth regulation	-----	-----	43
Mt1	Metallothionein 1 in mouse, human ortholog metallothionein 1 binds divalent heavy metals, alters the intracellular concentration of heavy metals in the cell	30, 31	-----	-----
Srebf1	Transcription factor, responsible for regulating lipid balance in liver	-----	97	-----

A list of the 21 genes having translational relevance that were found to be differentially expressed in both mTORC1 and mTORC2 knockout animals. Categories are listed for hepatocellular carcinoma, non-alcoholic fatty liver disease, and other human morbidities, and each gene is linked to articles that describe its role in one or more of the categories.

A.2 mTORC1 KO Hallmark gene set enrichments

Hallmark Collection of Gene Sets	NES	FDR q value
Bile Acid Metabolism	-2.08	0.004
Xenobiotic Metabolism	-1.8	0.064
Cholesterol Homeostasis	-1.71	0.096
E2F Targets	2.17	0.000
G2M Targets	2.08	0.001
Allograft Rejection	2.02	0.002
Interferon Gamma Response	1.86	0.014
TNF-a Signaling via NFkB	1.74	0.03

A.3 mTORC1 KO Kegg and Reactome gene set enrichments

Kegg and Reactome Collection of Gene Sets	NES	FDR q Value
Reactome cholesterol biosynthesis	-2.48	0
Reactome activation of gene expression by Srebf/Srebp	-2.14	0.087
Kegg Ribosome	2.47	0
Reactome nonsense mediated decay NMD independent of the exon junction complex EJC	2.43	0
Reactome eukaryotic translation initiation	2.36	0
Reactome SRP dependent cotranslational protein targeting to membrane	2.33	0
Reactome resolution of sister chromatid cohesion	2.16	0.003
Reactome rRNA processing in the nucleus and cytosol	2.15	0.003
Reactome influenza infection	2.13	0.005
Reactome selenoamino acid metabolism	2.09	0.008
Reactome regulation of expression of SLITS and ROBOS	2.06	0.012
Reactome immunoregulatory interactions between a lymphoid and a non-lymphoid cell	2.04	0.016
Reactome mitotic spindle checkpoint	2.04	0.016
Reactome DNA damage telomere stress induced senescence	2	0.03
Reactome interleukin 10 signaling	1.99	0.035
Reactome Rho GTPases Activate Formins	1.96	0.044
Reactome activation of the mRNA upon binding of the cap binding complex and subsequent binding to 43S	1.95	0.047
Reactome condensation of prophase chromosomes	1.9	0.076
Reactome nucleosome assembly	1.9	0.077
Kegg cytokine-cytokine receptor interaction	1.89	0.082
Reactome phosphorylation of the APC C	1.87	0.091

A.4 mTORC1 KO Gene Ontology gene set enrichments

Gene Ontology Collection of Gene Sets	NES	FDR q Value
GO_cytosolic_ribosome	2.4	0
GO_cotranslational_protein_targeting_to_membrane	2.4	0
GO_mitotic_sister_chromatid_segregation	2.36	0
GO_establishment_of_protein_localization_to_endoplasmic_reticulum	2.23	0.005
GO_mitotic_spindle_organization	2.17	0.015
GO_nuclear_transcribed_mrna_catabolic_process_nonsense_mediated_decay	2.15	0.017
GO_condensed_chromosome_centromeric_region	2.14	0.018
GO_positive_regulation_of_lymphocyte_migration	2.1	0.025
GO_mitotic_nuclear_division	2.09	0.027
GO_negative_regulation_of_metaphase_anaphase_transition_of_cell_cycle	2.07	0.035
GO_regulation_of_chromosome_segregation	2.07	0.035
GO_b_cell_receptor_signaling_pathway	2	0.08
GO_schwann_cell_development	2	0.085
GO_dna_replication_independent_nucleosome_organization	1.98	0.097

Shown above are GSEA enrichments for mTORC1 knockout RNA-seq shortlist data. An FDR q value of 0.1 or less and a normalized enrichment score (NES) ≤ -1.70 for negative enrichment and ≥ 1.70 for positive enrichment were used as selection criteria. All sets that met the cutoff are included here, and redundant gene sets were purged prior to assembly of final tables.

A.5 mTORC2 KO Reactome gene set enrichments

C2 Reactome Gene Set	NES	FDR q Value
KEGG_RIBOSOME	2.77	0
REACTOME_SRP_DEPENDENT_COTRANSLATIONAL_PROTEIN_TARGETING_TO_MEMBRANE	2.61	0.004
REACTOME_NONSENSE_MEDIATED_DECAY_NMD_INDEPENDENT_OF_THE_EXON_JUNCTION_COMPLEX_EJC	2.6	0.003
REACTOME_EUKARYOTIC_TRANSLATION_INITIATION	2.53	0.009
REACTOME_SELENOAMINO_ACID_METABOLISM	2.5	0.011
REACTOME_RRNA_PROCESSING	2.49	0.011
REACTOME_INFLUENZA_INFECTION	2.42	0.027

A.6 mTORC2 Gene Ontology gene set enrichments

C5 Ontology Gene Sets	NES	FDR q Value
GO_CYTOSOLIC_RIBOSOME	2.58	0.001
GO_COTRANSLATIONAL_PROTEIN_TARGETING_TO_MEMBRANE	2.47	0.034
GO_ESTABLISHMENT_OF_PROTEIN_LOCALIZATION_TO_ENDOPLASMIC_RETICULUM	2.44	0.03
GO_STRUCTURAL_CONSTITUENT_OF_RIBOSOME	2.43	0.035

Shown above are GSEA enrichments for mTORC2 knockout RNA-seq shortlist data. An FDR q value of 0.1 or less and a normalized enrichment score (NES) ≤ -1.70 for negative enrichment and ≥ 1.70 for positive enrichment were used as selection criteria. All sets that met the cutoff are included here, and redundant gene sets were purged prior to assembly of final tables.

A.7 List of common GSEA enrichments for mTORC1 and mTORC2 KO group

Enrichment ID	mTORC1		mTORC2	
	NES	FDR q Value	NES	FDR q Value
Kegg_ Ribosome	2.47	0	2.77	0
Reactome_ nonsense_ mediated_ decay_ NMD_independent_ of _the_ exon *junction* complex _EJC	2.43	0	2.60	0.003
Reactome _eukaryotic_ translation _initiation	2.36	0	2.53	0.009
Reactome_ SRP _dependent_ cotranslational protein targeting_ to _membrane	2.33	0	2.5	0.011
Reactome_Nonsense_Mediated_Decay_NMD	2.27	0	2.47	0.012
Reactome_ rRNA _processing _in_ the nucleus_ and _cytosol	2.15	0.003	2.48	0.012
Reactome_ rRNA _processing	2.11	0.007	2.49	0.011
Reactome_Influenza_Infection	2.13	0.005	2.42	0.027
Reactome_Selenoamino_Acid_Metabolism	2.09	0.008	2.5	0.011
GO_cytosolic_ribosome	2.4	0	2.58	0.001
GO_cytosolic_large_ribosomal_subunit	2.3	0.00093	2.51	0.023
GO_Cotranslational_Protein_Targeting_To_Membrane	2.4	0	2.47	0.034
GO_Cytosolic_Small_Ribosomal_Subunit	2.01	0.08	2.46	0.028

Shown above is a list of enriched categories that were found in both mTORC1 and mTORC2 knockout GSEA results. Identical selection criteria were used, and redundant results were purged prior to creation of the final table.

APPENDIX B

FIGURES

B.1 Metascape enrichments of mTORC1 KO shortlist data

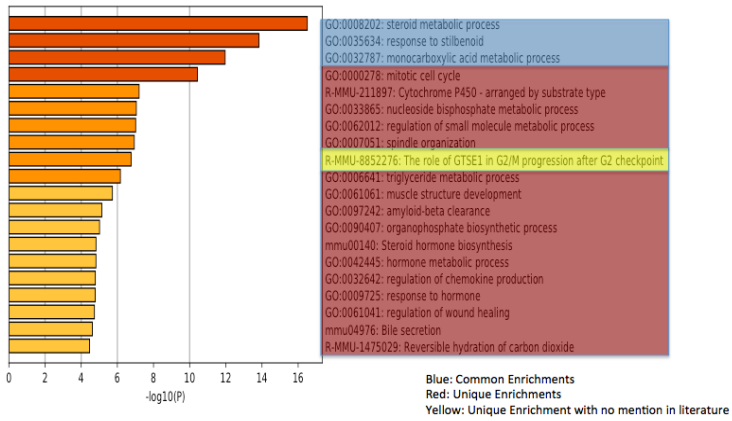

B.2 Metascape enrichments of mTORC2 KO shortlist data

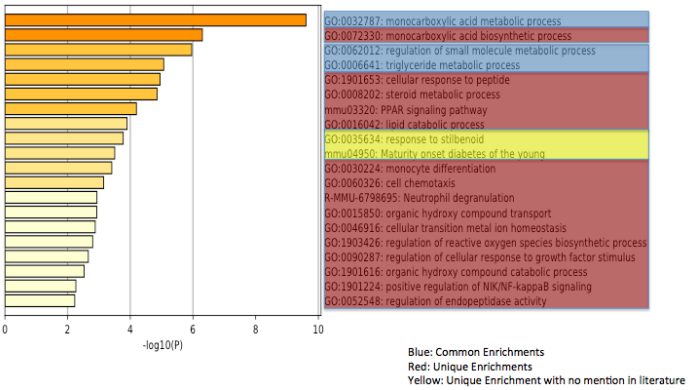

B.3 Metascape enrichments of 23 common genes

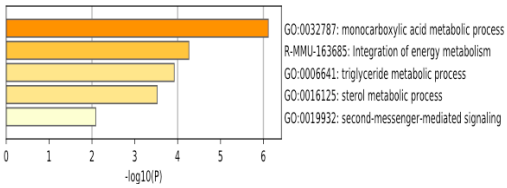

B.4 Venn diagram of mTORC1 and mTORC2 KO differentially expressed genes

B.5 RNA-seq analysis of Raptor and Rictor expression, and western immunoblot analysis of mTORC1 and mTORC2 experimental groups

	Gene	log2(Ratio)	q Value
mTORC1 KO	Rptor	-1.69	True
mTORC2 KO	Rictor	-0.31	False

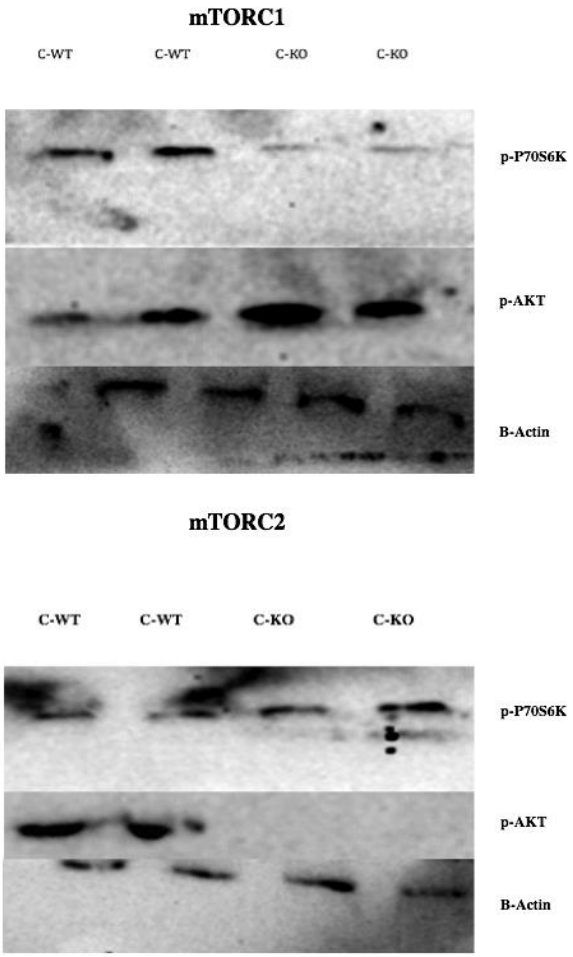

Metascape enrichments are shown above for mTORC1 in Figure B.1, and for mTORC2 in Figure B.2. Red indicates a unique enrichment, blue a common enrichment, and yellow an enrichment that is novel in its relationship to either mTORC1 or mTORC2. Metascape enrichments for the 23 genes differentially expressed in both mTORC1 and mTORC2 KO datasets are shown in Figure B.3. Figure B.4 provides a Venn diagram overview of the overlap between mTORC1 and mTORC2 knockout datasets, as well as the total number of genes differentially expressed in both complex's data sets. Immunoblots for mTORC1 and mTORC2 experimental groups are shown in Figure 1.e, with β-Actin loading controls used for both experimental groups. Loading of gels was completed in duplicate for WT and KO groups for both experiments. A complementary addition of Raptor and Rictor KO RNA-seq expression data is included as supplement.

B.6 IPA canonical pathway enrichments for mTORC1 KO

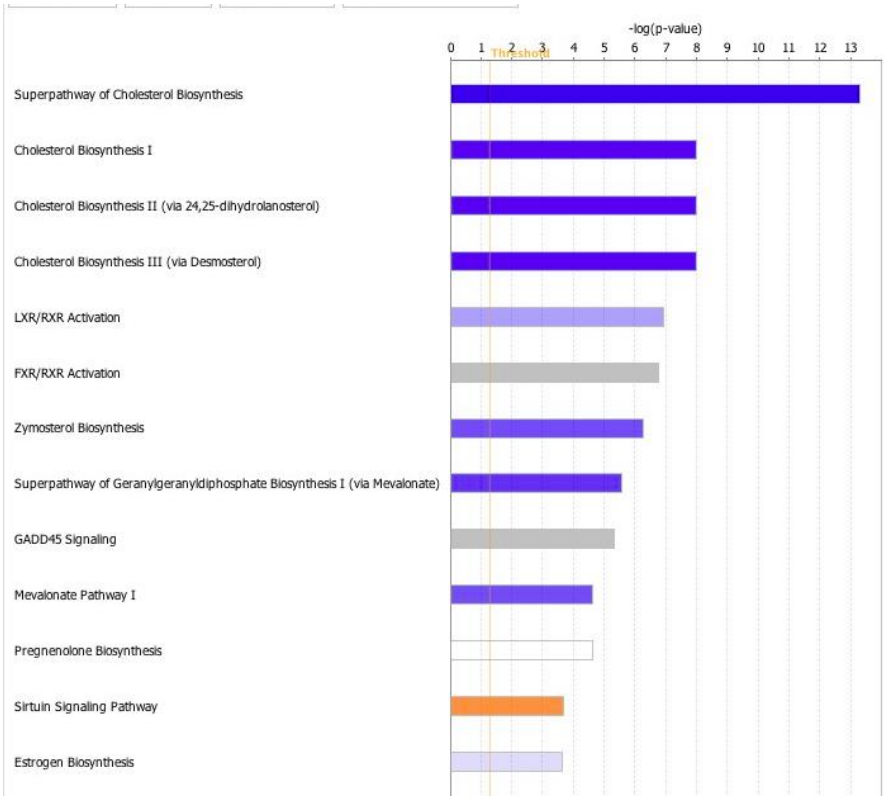

B.7 IPA disease enrichments for mTORC1 KO

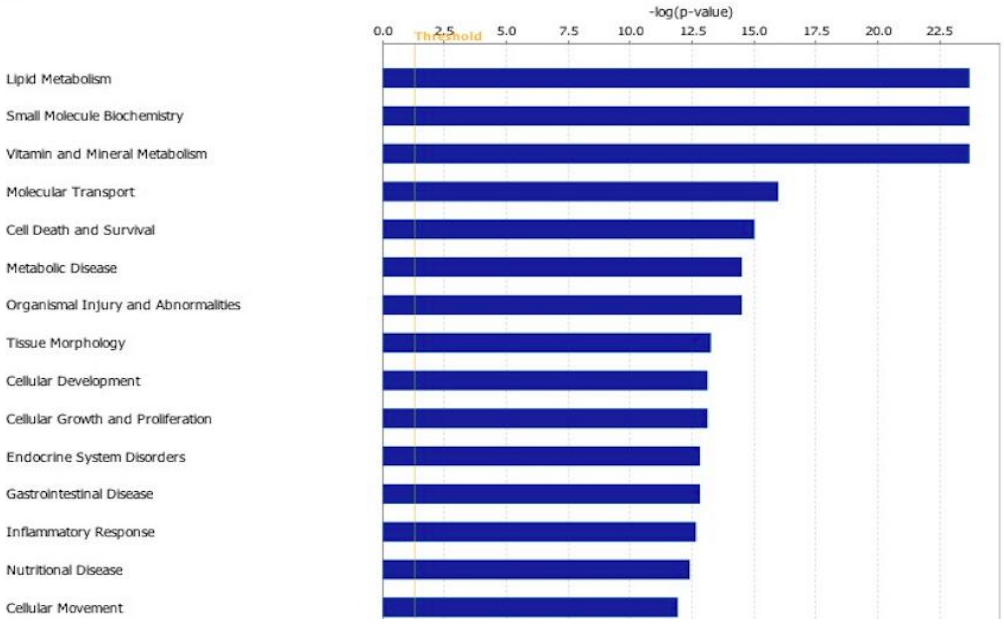

B.8 IPA canonical pathway enrichments for mTORC2 KO

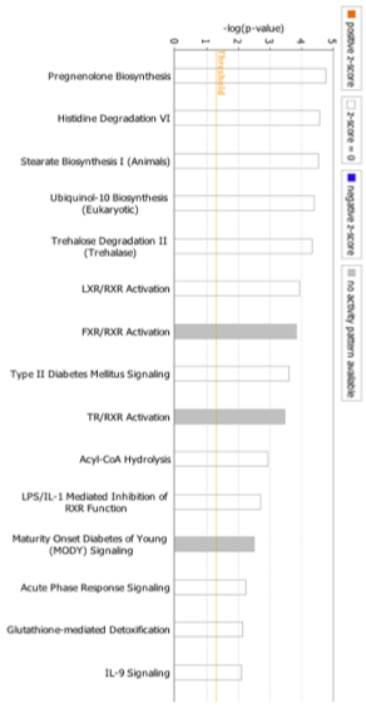

IPA readouts for enriched biological pathways and disease pathways for mTORC1 are shown in Figures B.6 and B.7, respectively. The top 15 enriched categories were used for both figures. IPA readouts for mTORC2 biological pathways and disease pathways are shown in Figures B.8 and B.9, respectively. Enrichment z scores are shown in orange for positive, blue for negative, white for zero, and grey if no activity relationship was calculated in IPA.

B.9 IPA disease enrichments for mTORC2 KO

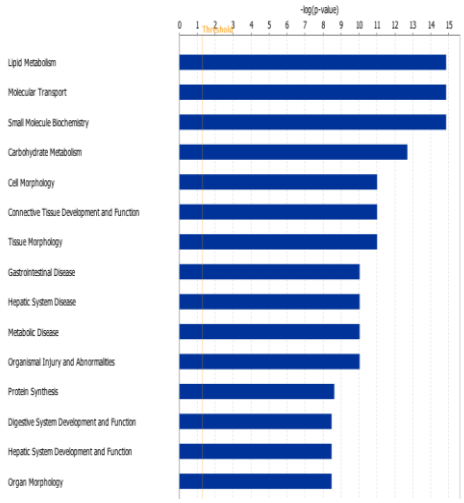

B.10 IPA upstream regulator analysis for mTORC1 KO

Upstream Regulator	Molecule Type	Predicted Activation St...	Activation z-s...	p-value of overlap	Target Molecules in Dataset
PPARA	ligand-dependent nuclear receptor	Activated	2.655	7.76E-37	↑Acot6, ↓ACSS2, ↑APOA4, ↓APOM, ↑AQP7, ↓AQP8, ↓ASL, ↓ASNS, ↑BCL2, ↑C... ...all 57
SREBF2	transcription regulator	Inhibited	-3.287	1.03E-25	↓AACS, ↓ACLY, ↓ACSS2, ↓ALDOC, ↑CDKN1A, ↓CYP51A1, ↓CYP7B1, ↓CYP8B1, ...all 24
SREBF1	transcription regulator	Inhibited	-2.428	3.56E-21	↓AACS, ↓ACLY, ↓ACSS2, ↓ALDOC, ↑BCL2, ↑CSAR1, ↑CDKN1A, ↓CSAD, ↓CYP... ...all 32
TP73	transcription regulator	Inhibited	-3.048	1.88E-13	↓ACTA2, ↑ATF3, ↑BCL2, ↑BIRC5, ↑BTG2, ↑CCNB1, ↑CD83, ↑CDK1, ↑CDKN... ...all 30
NCOA2	transcription regulator	Inhibited	-3.037	3.41E-13	↑ACOT1, ↑APOA4, ↓APOM, ↑CDKN1A, ↑CYP2B6, ↓CYP51A1, ↓EGR1, ↓FASN, ...all 17
STAT5B	transcription regulator	Inhibited	-2.674	2.39E-11	↑ACOT1, ↑BCL2, ↑CA2, ↑CDKN1A, ↑CYP2A6 (includes others), ↑Cyp2b13/C... ...all 23
HNF4A	transcription regulator	Inhibited	-2.056	2.41E-10	↓ABCB10, ↓ABCC3, ↓ACLY, ↑ACOT1, ↓ACSS2, ↓ACTA2, ↑AJUBA, ↑ANXA5, ↑... ...all 68
SIRT2	transcription regulator	Inhibited	-2.646	4.73E-09	↓AACS, ↓DHCR7, ↓HMGCR, ↓IDI1, ↓LSS, ↓MVD, ↓PMVK ...all 7
MYBL2	transcription regulator	Activated	2.770	1.45E-08	↑BCL2, ↑BIRC5, ↑CCNB1, ↑CDK1, ↑CENPE, ↑MYC, ↑PLK1, ↑TOP2A, ↑UBE2C ...all 9
RARA	ligand-dependent nuclear receptor	Activated	2.281	5.20E-08	↓APOM, ↑BIRC5, ↑CD84, ↑CD9, ↑CDK1, ↑CDKN1A, ↑CDKN3, ↑CENPF, ↑CTSS, ...all 21
FOXM1	transcription regulator	Activated	2.516	6.29E-08	↑BIRC5, ↑CCNB1, ↑CDK1, ↑CDKN1A, ↑CDKN3, ↑CENPE, ↑CENPF, ↑MKI67, ↑... ...all 13
CREB1	transcription regulator	Activated	2.280	2.09E-07	↑ATF3, ↑BCL2, ↑BIRC5, ↑BTG2, ↑CCNB1, ↑CD9, ↑CDKN1A, ↑CGREF1, ↑CYP... ...all 26
E2F3	transcription regulator	Activated	2.707	2.72E-07	↑BIRC5, ↑CCNB1, ↑CD9, ↑CDCA3, ↑CDK1, ↑CDKN1A, ↓ELF3, ↑IGF2, ↑LPL, ↓... ...all 14
MITF	transcription regulator	Activated	2.853	3.11E-07	↑BCL2, ↑CCNB1, ↑CDCA3, ↑CENPF, ↑CHKA, ↑GPNMB, ↑HAUS8, ↓IL6R, ↑LGA... ...all 16
JUN	transcription regulator	Activated	2.080	3.48E-07	↓ACTA2, ↓APOM, ↓ASNS, ↑ATF3, ↑C1QB, ↑CSAR1, ↑CDK1, ↑CDKN1A, ↓CYP... ...all 23
CDKN2A	transcription regulator	Inhibited	-2.080	1.40E-06	↓ACTA2, ↑BCL2, ↑BIRC5, ↑BTG2, ↑CAPG, ↑Ccl6, ↑CCNB1, ↑CDK1, ↑CDKN1A, ...all 17
HOXC8	transcription regulator	Activated	2.412	5.18E-06	↓GAS1, ↓GREM2, ↓KRT19, ↑Ly6a (includes others), ↑RARB, ↓SERPINF1 ...all 6
STAT1	transcription regulator	Activated	2.288	2.48E-04	↑BIRC5, ↑CDKN1A, ↑CTSS, ↓EGR1, ↑Ly6a (includes others), ↑MYC, ↑PLSCR1, ...all 15
ZFP36	transcription regulator	Inhibited	-2.592	2.77E-04	↑CD36, ↑CDKN1A, ↑CTSS, ↑CYBB, ↑NUF2, ↑PBK, ↑TOP2A ...all 7
MAF	transcription regulator	Inhibited	-2.425	3.76E-04	↓ACSS2, ↓CYP51A1, ↓HMGCR, ↓IDI1, ↓LSS, ↓PMVK ...all 6
KDM5B	transcription regulator	Inhibited	-2.273	7.38E-04	↑CCNB1, ↑CDCA3, ↑CDK1, ↓EGR1, ↑HMMR, ↑KIF2C, ↑PBK, ↑TOP2A ...all 8
NFKB2	transcription regulator	Activated	2.219	9.09E-04	↑ANXA5, ↑BCL2, ↑CD83, ↑CDKN1A, ↑CTSS, ↑MYC ...all 6
HOXA10	transcription regulator	Inhibited	-2.137	1.16E-03	↑CDKN1A, ↑CYBB, ↓HMGCR, ↑IDH2, ↑KLF10, ↑LEPR, ↑NR4A1, ↓PROM1, ↑RBP1... ...all 9
MTPN	transcription regulator	Activated	2.190	6.25E-03	↑BCL2, ↑CCNB1, ↑CDK1, ↑Mt1, ↑MYC ...all 5
TRIM24	transcription regulator	Inhibited	-2.219	1.41E-02	↑BLNK, ↑CA2, ↑LGALS3, ↑Ly6a (includes others), ↑USP18 ...all 5

B.11 IPA upstream regulator analysis for mTORC2 KO

Upstream Regulator	Molecule Type	Predicted Activation State	Activation z-score	p-value of overlap	Target Molecules in Dataset
RORA	ligand-dependent nuclear receptor	Inhibited	-2.219	2.84E-18	↑ABCD2, ↓CD36, ↑CISH, ↑CYP... ...all 17
STAT5B	transcription regulator	Inhibited	-2.052	1.98E-15	↑ABCD2, ↑ACOT1, ↓ACOT11, ↑.....all 17
MLX	transcription regulator	Inhibited	-2.207	1.48E-08	↓FASN, ↓MID1IP1, ↓PKLR, ↓SCD, ↑....all 5
PPARD	ligand-dependent nuclear receptor	Inhibited	-2.464	2.32E-08	↓CD36, ↓FASN, ↓GCK, ↑IGFBP2, ...all 10
NR1H3	ligand-dependent nuclear receptor	Inhibited	-2.432	2.64E-08	↓APCS, ↓CXCL2, ↓FASN, ↓GCK, ↑.....all 10
CEBPA	transcription regulator	Inhibited	-2.342	3.53E-08	↓FASN, ↓LCN2, ↑LEPR, ↓Mup1 ... ...all 13
ZBTB20	transcription regulator	Inhibited	-2.449	6.76E-08	↑CISH, ↓FASN, ↓GCK, ↑IGFBP2, ↑.....all 6
CEBPB	transcription regulator	Inhibited	-2.375	1.22E-06	↓APCS, ↓CXCL2, ↑INMT, ↓LCN2, ...all 11
ETV5	transcription regulator	Inhibited	-2.236	5.05E-05	↓FASN, ↓LCN2, ↓MID1IP1, ↓SCD, ↑....all 5
HNF1A	transcription regulator	Inhibited	-2.153	8.39E-04	↓APCS, ↓DCT, ↓FRK, ↓GCK, ↓Ml... ...all 8

B.12 STRING analysis of IPA upstream regulators for mTORC1 KO

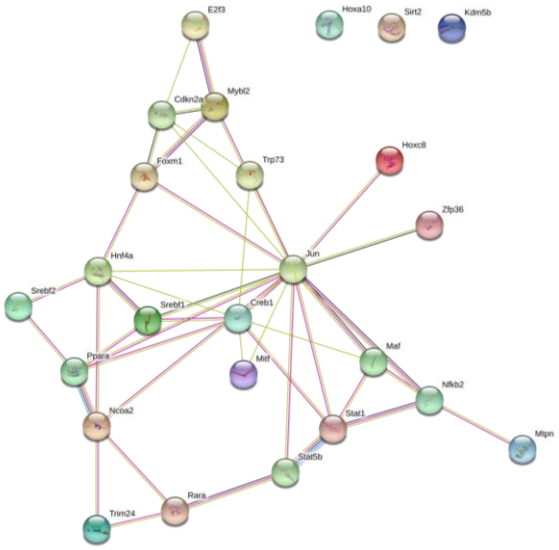

B.13 STRING analysis of IPA upstream regulators for mTORC2 KO

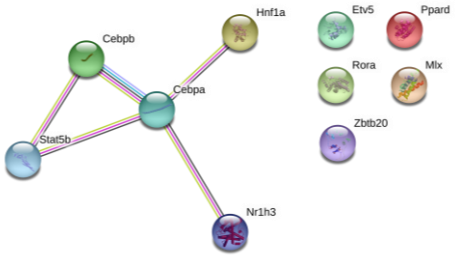

Upstream regulator analysis results are shown for
mTORC1 KO shortlist data in Figure B.10, and for mTORC2 shortlist data in Figure B.11. Upstream regulators are defined as those predicted by IPA to be upstream of the RNA-seq shortlist genes, and downstream of mTORC1 or mTORC2, respectively. Activation z-scores and p-values of overlap are listed for each upstream regulator, with orange indicating predicted activation and blue indicating predicted inactivation. STRING protein interaction networks are shown for mTORC1 upstream regulator analysis in Figure B.12, and for mTORC2 upstream regulator analysis in Figure B.13. Proteins with no calculated interaction or association relationship are shown as separate circles for mTORC1 in Figure B.12 and mTORC2 in Figure B.13.

B.14 mTORC1 downstream signaling pathway based on IPA results

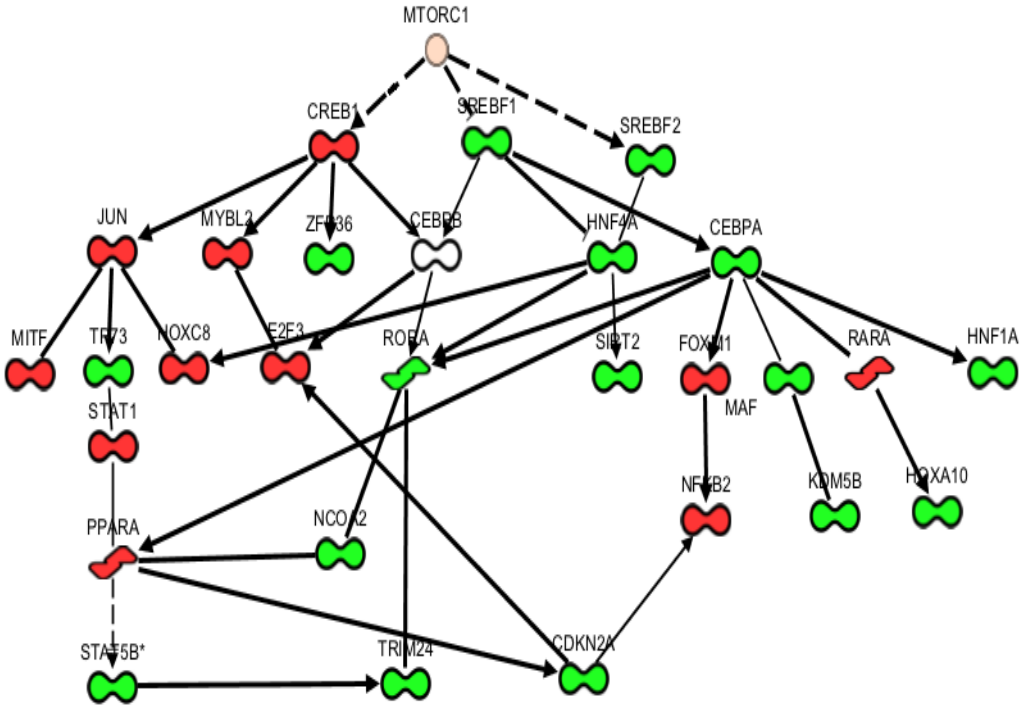

Figure B.15 mTORC2 downstream signaling pathway based on IPA results

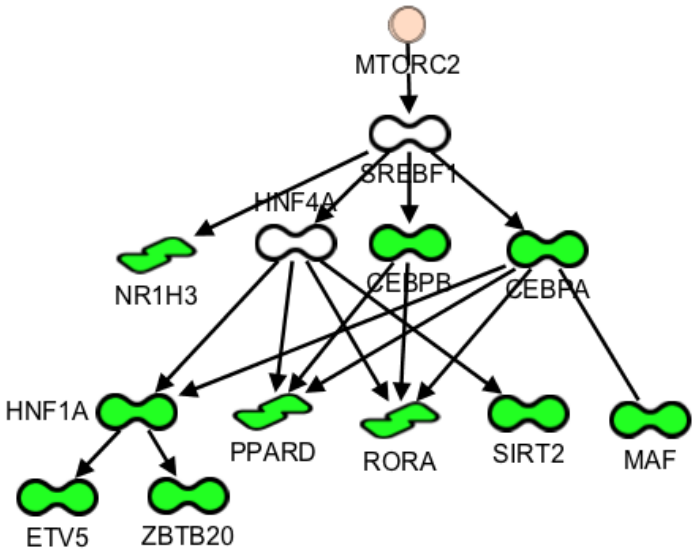

The predicted signaling downstream of mTORC1 and mTORC2 is shown above in Figures B.14 and B.15, respectively. Green indicates activation, and red indicates inactivation, with white indicating an indirect relationship. These figures display **active** mTOR signaling through the upstream regulators described in Figure B.10 and B.11. The activation status of upstream regulators in **inactive** mTOR signaling is the exact opposite of what is found in active signaling, with green indicating inactivation and red indicating activation in that scenario.

APPENDIX C

SUPPLEMENTAL ANNOTATION OF GENES

Genes Involved in Hepatocellular Carcinoma/Liver Cancer:

Fatty acid synthase (Fasn) was found to be critical in the abrogation of HCC progression in mice that had Akt dependent HCC, as evidenced by HCC progression in mice with KO Fasn (20).

For Myc, a recent study noted that in hepatocellular carcinoma, p53 mutant cancers that are addicted to Myc stabilization and driven by KRas are treatable by inhibition of Myc stabilization by AURKA (21).

Gna14 was found to be a hub gene for HCC, and may also play a role as a tumor marker for diagnosis, staging, and treatment of HCC (22).

Cyp26a1, one of the many cytochrome genes, was downregulated in expression in an HCC cell line treated with non-toxic levels of a soybean flavone for 12 hours (23).

Extl1 was found to be upregulated and differentially methylated in C3H mice, serving as a model for HCC progression (24).

Research on the physiological role of CD36 has implicated it in the development of HCC, with the proposed mechanism being increased transport of free fatty acids into the liver leading to an epithelial-mesenchymal transition, thereby promoting HCC metastasis (25).

Saa2 was found in the blood sera of a sample of 31 patients with HCC, indicating that it could serve as a biomarker for the condition (26). Additionally, it was found to be decreased upon insulin treatment of hepatoma cell line, assumed to be an inflammatory response gene due to its association with IL-6 signaling (27). The same research group that proposed Saa2 as an inflammatory response gene also found that small molecule activation of AMP-activated protein

kinase (AMPK) repressed IL-6 signaling and the pro-inflammatory molecule Saa2, indicating that AMPK is a master regulator of inflammatory and metabolic pathways in hepatocytes, among them Saa2 (28).

Mir671, a microRNA, was found to be upregulated in samples of microvesicles, a type of extracellular vesicle released from the cell membrane, from patients with HCC (29).

Mt1, a metallothionein, was found to be downregulated in in human HCC samples, opening for the possibility of its use as a biomarker (30). It was also found that loss of nuclear expression of Mt1 was associated with a poor prognosis for HCC in a sample of 370 patients with the disease (31).

Research on cirrhotic liver samples that were also infected with hepatitis C showed that the most common mutation was in the leptin receptor gene. This held true for both tumor and non-tumor cirrhotic liver samples, indicating that accumulation of mutations in the LEPR gene and may lead to hepatocellular carcinoma characterized by altered LEPR signaling (32).

Genes Involved in NAFLD/Fatty Liver:

Rgs16, known as the Regulator of G-protein signaling 16, was found in a recent study to be responsible for development of fatty liver in mice that had transgenic Rgs16 introduced into their hepatocytes, which was connected to a tetracycline-sensitive promoter. Mice that were fed with doxycycline, a type of tetracycline antibiotic, in their water subsequently developed fatty liver deposits (33).

For the two Acot (Acyl-CoA thioesterase) genes, a knockdown of Acot1 in mouse hepatocytes resulted in increased hepatic oxidative stress and inflammation, both a hallmark of NAFLD (34). Interestingly, a knockdown of the same gene in mice with diet-induced hepatic steatosis resulted in a liver lipid content similar to controls, showing that while knockdown alone

could result in oxidative stress and inflammation, knockdown may also play a protective role against diet-inducted hepatic steatosis (34). The role of Acot2 was significantly less researched, however, a recent report in the literature noted that its likely role was functioning as an enhancer of fatty acid oxidation in the mitochondria, the likely mechanism being prevention of chemical intermediate accumulation in the mitochondrial matrix (35)

Serpina12, known commonly as Vaspin, was found to be positively associated with inflammation, serum glucose levels, and insulin resistance in a pool of patients with NAFLD (36).

CD36, the only gene found with research suggesting its role in both HCC and NAFLD, with previous research in our lab suggesting a reprogramming of liver lipid metabolism in offspring upon treatment of mice with the flame retardant PBDE-47 during gestation. This relationship was noted to be multidirectional- in low doses of PBDE-47, CD-36 expression decreased, and subsequently blood lipid levels increase, while moderate doses lead to increased CD36 expression and histological liver changes consistent with NAFLD (37).

In the B cells of the Pancreas, ChREBP regulates the expression of multiple lipogenic genes, among them Mid1ip1. It was found to be both necessary and sufficient to induce the expression of 15 lipogenic genes, and the function of Mid1ip1 appears to be upregulation of Acaca, an enzyme that catalyzes the carboxylation of acetyl-CoA to Malonyl-CoA (38).

Finally, Srebp1-c, the protein product of the Srebf1 gene, was found to induce fatty liver development in mice with a albumin promoter controlled overexpression of Srebf1, indicating that NAFLD may be mediated by increased Srebf1 signaling.

Genes Functioning in other Human Diseases:

A genome-wide analysis of mice that had significant atherosclerotic lesion formation found that the H2 major histocompatibility locus contained 12 candidate genes, among them Adgrf1, that were significantly associated with coronary heart disease. This indicates that Adgrf1 may mediate the inflammation that promotes atherosclerosis (39).

Chpf2 was found to be one of the several chondroitin sulfate-linked genes that were found to be mutated in 1/3 of a sample of 26 patients who had experienced a thrombotic storm, a rare type of clotting event that is characterized by severe, acute multiple clotting events often affecting young adults (40).

Dpy19l3 was recently discovered to function in c-mannosylation, a rare type of protein glycosylation (41). Its target protein, RPE-spondin, was found to be expressed at high levels in certain colon cancer cell lines, implicating RPE-spondin, and its putative regulator, Dpy19l3 (42).

In other works, Gpc1 was recently found to be associated with susceptibility to biliary atresia, a rare childhood disorder of the biliary tree that results in end stage hepatic disease (43).

Agpat9, part of a group of related proteins that acylate lysophosphatidic acid at an Sn2 position to produce phosphatidic acid, was initially discovered and found to be expressed in lung and spleen tissue, with its hypothesized role being synthesis of triglycerides and phospholipids in these tissues (44). Interestingly, recent research on the antimetabolite antineoplastic agent 5-azacytidine, used to prolong life in patients with acute myeloid leukemia, noted that significant upregulation in Agpat9 expression, mediated by the inhibitory effect 5-azacytidine displays on UMP (45). Together, these observations led to a conclusion that 5-azacytidine reprograms lipid metabolism in an epigenetic manner via hypomethylation of DNA, and that Agpat9 disruption,

along with UMP inhibition, is a possible mechanism of increased lipogenesis observed in the patient cohort (44,45).

REFERENCES

1. Boylan, J. M., Sanders, J. A., Neretti, N., & Gruppuso, P. A. (2015). Profiling of the fetal and adult rat liver transcriptome and translatome reveals discordant regulation by the mechanistic target of rapamycin (mTOR). *American Journal of Physiology-Regulatory, Integrative and Comparative Physiology*,*309*(1). doi:10.1152/ajpregu.00114.2015

2. Wullschleger, S., Loewith, R., & Hall, M. N. (2006). TOR Signaling in Growth and Metabolism. *Cell*,*124*(3), 471-484. doi:10.1016/j.cell.2006.01.016

3. Sarbassov DD, Ali SM, Kim DH, Guertin DA, Latek RR, Erdjument-Bromage H, Tempst P, Sabatini DM (Jul 2004). "Rictor, a novel binding partner of mTOR, defines a rapamycin-insensitive and raptor-independent pathway that regulates the cytoskeleton". *Current Biology*. **14** (14): 1296–302

4. Oh, W. J., & Jacinto, E. (2011). MTOR complex 2 signaling and functions. *Cell Cycle*,*10*(14), 2305-2316. doi:10.4161/cc.10.14.16586

5. Zhang, Y., Jia, Q., Kadel, D., Zhang, X., & Zhang, Q. (2018). Targeting mTORC1/2 Complexes Inhibit Tumorigenesis and Enhance Sensitivity to 5-Flourouracil (5-FU) in Hepatocellular Carcinoma: A Preclinical Study of mTORC1/2-Targeted Therapy in Hepatocellular Carcinoma (HCC). *Medical Science Monitor*,*24*, 2735-2743. doi:10.12659/msm.907514

6. Menon, S., Yecies, J. L., Zhang, H. H., Howell, J. J., Nicholatos, J., Harputlugil, E., . . . Manning, B. D. (2012). Chronic Activation of mTOR Complex 1 Is Sufficient to Cause Hepatocellular Carcinoma in Mice. *Science Signaling*,*5*(217). doi:10.1126/scisignal.2002739

7. Lee, Y. S., Park, J. S., Lee, D. H., Lee, D., Kwon, S. W., Lee, B., & Bae, S. H. (2018). The Antidiabetic Drug Lobeglitazone Protects Mice From Lipogenesis-Induced Liver Injury via Mechanistic Target of Rapamycin Complex 1 Inhibition. *Frontiers in Endocrinology*,*9*. doi:10.3389/fendo.2018.00539

8. Younossi ZM, Koenig AB, Abdelatif D, Fazel Y, Henry L, Wymer M (July 2016). "Global epidemiology of nonalcoholic fatty liver disease-Meta-analytic assessment of prevalence, incidence, and outcomes". *Hepatology*. **64** (1): 73–84

9. Liu, J., Ling Ma, K., Zhang, Y., Wu, Y., Bo Hu, Z., Li Lv, L., . . . Chen Liu, B. (2015). Activation of mTORC1 disrupted LDL receptor pathway: A potential new mechanism for the progression of non-alcoholic fatty liver disease. *The International Journal of Biochemistry & Cell Biology*,*61*, 8-19. Retrieved August 17, 2019.

10. Lamming, D. W., Demirkan, G., Boylan, J. M., Mihaylova, M. M., Peng, T., Ferreira, J., … Gruppuso, P. A. (2014). Hepatic signaling by the mechanistic target of rapamycin complex 2 (mTORC2). *FASEB journal : official publication of the Federation of American Societies for Experimental Biology*, *28*(1), 300–315. doi:10.1096/fj.13-237743

11. Kim, L. C., Cook, R. S., & Chen, J. (2017). mTORC1 and mTORC2 in cancer and the tumor microenvironment. *Oncogene*, *36*(16), 2191–2201. doi:10.1038/onc.2016.363

12. Lien, E. C., Dibble, C. C., & Toker, A. (2017). PI3K signaling in cancer: beyond AKT. *Current opinion in cell biology*, *45*, 62–71. doi:10.1016/j.ceb.2017.02.007

13. Gan, X., Wang, J., Su, B., & Wu, D. (2011). Evidence for direct activation of mTORC2 kinase activity by phosphatidylinositol 3,4,5-trisphosphate. *The Journal of biological chemistry*, *286*(13), 10998–11002. doi:10.1074/jbc.M110.195016

14. Kim D, Pertea G, Trapnell C, Pimentel H, Kelley R, Salzberg SL. TopHat2: accurate alignment of transcriptomes in the presence of insertions, deletions and gene fusions. *Genome Biol.* 2013;**14**(4):R36.

15. Trapnell C, Hendrickson DG, Sauvageau M, Goff L, Rinn JL, Pachter L. Differential analysis of gene regulation at transcript resolution with RNA-seq. Nat Biotechnol. 2013;31(1):46–53.

16. Subramanian, A., Tamayo, P., Mootha, V. K., Mukherjee, S., Ebert, B. L., Gillette, M. A., … Mesirov, J. P. (2005). Gene set enrichment analysis: a knowledge-based approach for interpreting genome-wide expression profiles. *Proceedings of the National Academy of Sciences of the United States of America*, *102*(43), 15545–15550. doi:10.1073/pnas.0506580102

17. Zhou, Y., Zhou, B., Pache, L., Chang, M., Khodabakhshi, A. H., Tanaseichuk, O., … Chanda, S. K. (2019). Metascape provides a biologist-oriented resource for the analysis of systems-level datasets. *Nature communications*, *10*(1), 1523. doi:10.1038/s41467-019-09234-6

18. Zar, J.H. Biostatistical Analysis 1999 4th edn., NJ Prentice Hall, pp. 523.

19. Mischke, M., Pruis, M. G., Boekschoten, M. V., Groen, A. K., Fitri, A. R., Bert J. M. Van De Heijning, . . . Steegenga, W. T. (2013). Maternal Western-Style High Fat Diet Induces Sex-Specific Physiological and Molecular Changes in Two-Week-Old Mouse Offspring. *PLoS ONE,8*(11). doi:10.1371/journal.pone.0078623

20. Calvisi, D., Li, L., Pilo, G., Cigliano, A., Ribback, S., Dombrowski, F., . . . Evert, M. (2015). Inactivation of fatty acid synthase impairs hepatocarcinogenesis driven by AKT in mice. *Zeitschrift Für Gastroenterologie,53*(12). doi:10.1055/s-0035-1568081

21. Dauch, D., Rudalska, R., Cosso, G., Nault, J., Kang, T., Wuestefeld, T., . . . Zender, L. (2016). A MYC-aurora kinase A protein complex represents an actionable drug target in p53-altered liver cancer. *Nature Medicine,22*, 744-753.

22. Cai, C., Wang, W., & Tu, Z. (2019). Aberrantly DNA Methylated-Differentially Expressed Genes and Pathways in Hepatocellular Carcinoma. *Journal of Cancer,10*(2), 355-366. doi:10.7150/jca.27832

23. Lepri, S. R., Sartori, D., Semprebon, S. C., Baranoski, A., Coatti, G. C., & Mantovani, M. S. (2018). Genistein Affects Expression of Cytochrome P450 (CYP450) Genes in Hepatocellular Carcinoma (HEPG2/C3A) Cell Line. *Drug Metabolism Letters,12*(2), 138-144. doi:10.2174/1872312812666180709150440

24. Matsushita, J., Okamura, K., Nakabayashi, K., Suzuki, T., Horibe, Y., Kawai, T., . . . Nohara, K. (2018). The DNA methylation profile of liver tumors in C3H mice and identification of differentially methylated regions involved in the regulation of tumorigenic genes. *BMC Cancer,18*(1). doi:10.1186/s12885-018-4221-0

25. Nath, A., Li, I., Roberts, L. R., & Chan, C. (2015). Elevated free fatty acid uptake via CD36 promotes epithelial-mesenchymal transition in hepatocellular carcinoma. *Scientific Reports,5*(1). doi:10.1038/srep14752

26. Wahab, A. H., El-Halawany, M. S., Emam, A. A., Elfiky, A., & Elmageed, Z. Y. (2016). Identification of circulating protein biomarkers in patients with hepatocellular carcinoma concomitantly infected with chronic hepatitis C virus. *Biomarkers,*1-8. doi:10.1080/1354750x.2016.1252966

27. Wallerstedt, E., Sandqvist, M., Smith, U., & Andersson, C. X. (2011). Anti-inflammatory effect of insulin in the human hepatoma cell line HepG2 involves decreased transcription of IL-6 target genes and nuclear exclusion of FOXO1. *Molecular and Cellular Biochemistry,352*(1-2), 47-55. doi:10.1007/s11010-011-0738-0

28. Nerstedt, A., Cansby, E., Amrutkar, M., Smith, U., & Mahlapuu, M. (2013). Pharmacological activation of AMPK suppresses inflammatory response evoked by IL-6 signalling in mouse liver and in human hepatocytes. *Molecular and Cellular Endocrinology,375*(1-2), 68-78. doi:10.1016/j.mce.2013.05.013

29. Sun, L., Xiong, W., Chen, X., Yi, X., Li, H., & Jie, S. (2013). 1054 Circulating Microvesicles Micrornas Expression Profiles In Hepatocellular Carcinoma. *Journal of Hepatology*, *58*. doi: 10.1016/s0168-8278(13)61055-7

30. Li, H., Lu, Y., Chen, H., & Liu, J. (2016). Dysregulation of metallothionein and circadian genes in human hepatocellular carcinoma. *Chronobiology International,34*(2), 192-202. doi:10.1080/07420528.2016.1256300

31. Park, Y., & Yu, E. (2013). Expression of metallothionein-1 and metallothionein-2 as a prognostic marker in hepatocellular carcinoma. *Journal of Gastroenterology and Hepatology,28*(9), 1565-1572. doi:10.1111/jgh.12261

32. Ikeda, A., Shimizu, T., Matsumoto, Y., Fujii, Y., Eso, Y., Inuzuka, T., . . . Marusawa, H. (2014). Leptin Receptor Somatic Mutations Are Frequent in HCV-Infected Cirrhotic Liver and Associated With Hepatocellular Carcinoma. *Gastroenterology,146*(1). doi:10.1053/j.gastro.2013.09.025

33. Pashkov, V., Huang, J., Parameswara, V. K., Kedzierski, W., Kurrasch, D. M., Tall, G. G., . . . Wilkie, T. M. (2011). Regulator of G Protein Signaling (RGS16) Inhibits Hepatic Fatty Acid Oxidation in a Carbohydrate Response Element-binding Protein (ChREBP)-dependent Manner. *Journal of Biological Chemistry,286*(17), 15116-15125. doi:10.1074/jbc.m110.216234

34. Franklin, M. P., Sathyanarayan, A., & Mashek, D. G. (2017). Acyl-CoA Thioesterase 1 (ACOT1) Regulates PPARα to Couple Fatty Acid Flux With Oxidative Capacity During Fasting. *Diabetes,66*(8), 2112-2123. doi:10.2337/db16-1519

35. Moffat, Cynthia, et al. "Acyl-CoA Thioesterase-2 Facilitates Mitochondrial Fatty Acid Oxidation in the Liver." *Journal of Lipid Research*, vol. 55, no. 12, Nov. 2014, pp. 2458–2470., doi:10.1194/jlr.m046961.

36. Aliasghari, F., Izadi, A., Jabbari, M., Imani, B., Gargari, B. P., Asjodi, F., & Ebrahimi, S. (2018). Are Vaspin and Omentin-1 Related to Insulin Resistance, Blood Pressure and Inflammation in NAFLD Patients? *Journal of Medical Biochemistry,0*(0). doi:10.1515/jomb-2018-0006

37. Khalil, A., Parker, M., Mpanga, R., Cevik, S. E., Thorburn, C., & Suvorov, A. (2017). Developmental Exposure to 2,2′,4,4′–Tetrabromodiphenyl Ether Induces Long-Lasting Changes in Liver Metabolism in Male Mice. *Journal of the Endocrine Society,1*(4), 323-344. doi:10.1210/js.2016-1011

38. Sae-Lee, C., Moolsuwan, K., Chan, L., & Poungvarin, N. (2016). ChREBP Regulates Itself and Metabolic Genes Implicated in Lipid Accumulation in β–Cell Line. *Plos One,11*(1). doi:10.1371/journal.pone.0147411

39. Grainger, A. T., Jones, M. B., Li, J., Chen, M., Manichaikul, A., & Shi, W. (2016). Genetic analysis of atherosclerosis identifies a major susceptibility locus in the major histocompatibility complex of mice. *Atherosclerosis,254*, 124-132. doi:10.1016/j.atherosclerosis.2016.10.011

40. Nuytemans, K., Ortel, T. L., Gomez, L., Hofmann, N., Alves, N., Dueker, N., . . . Vance, J. M. (2018). Variants in chondroitin sulfate metabolism genes in thrombotic storm. *Thrombosis Research,161*, 43-51. doi:10.1016/j.thromres.2017.11.016

41. Niwa, Y., Suzuki, T., Dohmae, N., & Simizu, S. (2016). Identification of DPY19L3 as the C-mannosyltransferase of R-spondin1 in human cells. *Molecular Biology of the Cell,27*(5), 744-756. doi:10.1091/mbc.e15-06-0373

42. Morishita, S., Suzuki, T., Niwa, Y., Dohmae, N., & Simizu, S. (2017). Dpy-19 like 3-mediated C-mannosylation and expression levels of RPE-spondin in human tumor cell lines. *Oncology Letters,14*(2), 2537-2544. doi:10.3892/ol.2017.6465

43. Cui, S., Leyva–Vega, M., Tsai, E. A., Eauclaire, S. F., Glessner, J. T., Hakonarson, H., . . . Matthews, R. P. (2013). Evidence From Human and Zebrafish That GPC1 Is a Biliary Atresia Susceptibility Gene. *Gastroenterology,144*(5). doi:10.1053/j.gastro.2013.01.022

44. Agarwal, A. K, et al. "Functional Characterization of Human 1-Acylglycerol-3-Phosphate-O-Acyltransferase Isoform 9: Cloning, Tissue Distribution, Gene Structure, and Enzymatic Activity." *Journal of Endocrinology*, vol. 193, no. 3, Jan. 2007, pp. 445–457., doi:10.1677/joe-07-0027

45. Poirier, Steve, et al. "The Epigenetic Drug 5-Azacytidine Interferes with Cholesterol and Lipid Metabolism." *Journal of Biological Chemistry*, vol. 289, no. 27, 2014, pp. 18736–18751., doi:10.1074/jbc.m114.563650.

46. Inoki, K., Li, Y., Zhu, T., Wu, J., & Guan, K.-L. (2002). TSC2 is phosphorylated and inhibited by Akt and suppresses mTOR signalling. *Nature Cell Biology*, *4*(9), 648–657. doi: 10.1038/ncb839

47. Potter CJ, Pedraza LG, Xu T. Akt regulates growth by directly phosphorylating Tsc2. Nat Cell Biol. 2002 Sep;4(9):658–65.

48. Manning BD, Tee AR, Logsdon MN, Blenis J, Cantley LC. Identification of the Tuberous Sclerosis Complex-2 Tumor Suppressor Gene Product Tuberin as a Target of the Phosphoinositide 3-Kinase/Akt Pathway. Mol Cell. 2002;10(1):151–62

49. Inoki K, Li Y, Xu T, Guan K-L. Rheb GTPase is a direct target of TSC2 GAP activity and regulates mTOR signaling. Genes Dev. 2003 Aug 1;17(15):1829–34

50. Tee AR, Manning BD, Roux PP, Cantley LC, Blenis J. Tuberous Sclerosis Complex Gene Products, Tuberin and Hamartin, Control mTOR Signaling by Acting as a GTPase-Activating Protein Complex toward Rheb. Curr Biol. 2003;13(15):1259–68.

51. Humphrey SJ, Yang G, Yang P, Fazakerley DJ, Stöckli J, Yang JY, et al. Dynamic adipocyte phosphoproteome reveals that Akt directly regulates mTORC2. Cell Metab. 2013 Jun 4;17(6):1009–20.

52. Yang G, Murashige DS, Humphrey SJ, James DE. A Positive Feedback Loop between Akt and mTORC2 via SIN1 Phosphorylation. Cell Rep. 2015 Jul 29;12(6):937–43

53. Liu P, Gan W, Inuzuka H, Lazorchak AS, Gao D, Arojo O, et al. Sin1 phosphorylation impairs mTORC2 complex integrity and inhibits downstream Akt signalling to suppress tumorigenesis. Nat Cell Biol. Nature Publishing Group, a division of Macmillan Publishers Limited. All Rights Reserved. 2013 Nov;15(11):1340–50

54. Baar, E. L., Carbajal, K. A., Ong, I. M., & Lamming, D. W. (2016). Sex- and tissue-specific changes in mTOR signaling with age in C57BL/6J mice. *Aging cell*, *15*(1), 155–166. doi:10.1111/acel.12425

55. Alberts B, Johnson A, Lewis J, et al. Molecular Biology of the Cell. 4th edition. New York: Garland Science; 2002. Innate Immunity. Available from: https://www.ncbi.nlm.nih.gov/books/NBK26846/

56. Jones, R. G., & Pearce, E. J. (2017). MenTORing Immunity: mTOR Signaling in the Development and Function of Tissue-Resident Immune Cells. *Immunity*, *46*(5), 730–742. doi:10.1016/j.immuni.2017.04.028

57. Linke, M., Fritsch, S. D., Sukhbaatar, N., Hengstschläger, M., & Weichhart, T. (2017). mTORC1 and mTORC2 as regulators of cell metabolism in immunity. *FEBS letters*, *591*(19), 3089–3103. doi:10.1002/1873-3468.12711

58. Laplante, M., & Sabatini, D. M. (2009). An emerging role of mTOR in lipid biosynthesis. *Current biology : CB*, *19*(22), R1046–R1052. doi:10.1016/j.cub.2009.09.058

59. Dan, H. C., Cooper, M. J., Cogswell, P. C., Duncan, J. A., Ting, J. P., & Baldwin, A. S. (2008). Akt-dependent regulation of NF-{kappa}B is controlled by mTOR and Raptor in association with IKK. *Genes & development*, *22*(11), 1490–1500. doi:10.1101/gad.1662308

60. Janeway CA Jr, Travers P, Walport M, et al. Immunobiology: The Immune System in Health and Disease. 5th edition. New York: Garland Science; 2001. Principles of innate and adaptive immunity. Available from: https://www.ncbi.nlm.nih.gov/books/NBK27090/

61. Chiang J. Y. (2013). Bile acid metabolism and signaling. *Comprehensive Physiology*, *3*(3), 1191–1212. doi:10.1002/cphy.c120023

62. Laplane, M., Sabatini, D., mTOR signaling at a glance Journal of Cell Science 2009 122: 3589-3594; doi: 10.1242/jcs.051011

63. Li, J., Kim, S. G., & Blenis, J. (2014). Rapamycin: one drug, many effects. *Cell metabolism*, *19*(3), 373–379. doi:10.1016/j.cmet.2014.01.001

64. Demirkan G., Yu K., Boylan J. M., Salomon A. R., Gruppuso P. A. (2011) Phosphoproteomic profiling of in vivo signaling in liver by the mammalian target of rapamycin complex 1 (mtorc1). PLoS One 6, e21729.

65. Hsu P. P., Kang S. A., Rameseder J., Zhang Y., Ottina K. A., Lim D., Peterson T. R., Choi Y., Gray N. S., Yaffe M. B., Marto J. A., Sabatini D. M. (2011) The mtor-regulated phosphoproteome reveals a mechanism of mtorc1-mediated inhibition of growth factor signaling. Science 332, 1317–1322

66. Causal analysis approaches in Ingenuity Pathway Analysis. Bioinformatics. 2014 Feb 15;30(4):523-30.

67. Wallace, M. C., Preen, D., Jeffrey, G. P., & Adams, L. A. (2015). The evolving epidemiology of hepatocellular carcinoma: a global perspective. *Expert review of gastroenterology & hepatology*, *9*(6), 765–779. doi:10.1586/17474124.2015.1028363

68. El-Serag, H. B., & Rudolph, K. L. (2007). Hepatocellular carcinoma: epidemiology and molecular carcinogenesis. *Gastroenterology*, *132*(7), 2557–2576. doi:10.1053/j.gastro.2007.04.061

69. Zoller, H., & Tilg, H. (2016). Nonalcoholic fatty liver disease and hepatocellular carcinoma. *Metabolism: clinical and experimental*, *65*(8), 1151–1160. doi:10.1016/j.metabol.2016.01.010

70. Weiß, J., Rau, M., & Geier, A. (2014). Non-alcoholic fatty liver disease: epidemiology, clinical course, investigation, and treatment. *Deutsches Arzteblatt international*, *111*(26), 447–452. doi:10.3238/arztebl.2014.0447

71. Anderson, E. L., Howe, L. D., Jones, H. E., Higgins, J. P., Lawlor, D. A., & Fraser, A. (2015). The Prevalence of Non-Alcoholic Fatty Liver Disease in Children and Adolescents: A Systematic Review and Meta-Analysis. *PloS one, 10*(10), e0140908. doi:10.1371/journal.pone.0140908

72. Erridge, S., Pucher, P. H., Markar, S. R., Malietzis, G., Athanasiou, T., Darzi, A., … Jiao, L. R. (2017). Meta-analysis of determinants of survival following treatment of recurrent hepatocellular carcinoma. *The British journal of surgery*, *104*(11), 1433–1442. doi:10.1002/bjs.10597

73. Ikeda, M., Morizane, C., Ueno, M., Okusaka, T., Ishii, H., & Furuse, J. (2018). Chemotherapy for hepatocellular carcinoma: current status and future perspectives. *Japanese journal of clinical oncology*, *48*(2), 103–114. doi:10.1093/jjco/hyx180

74. Llovet, J. M., Ricci, S., Mazzaferro, V., Hilgard, P., Gane, E., Blanc, J. F., … SHARP Investigators Study Group (2008). Sorafenib in advanced hepatocellular carcinoma. *The New England journal of medicine*, *359*(4), 378–390. doi:10.1056/NEJMoa0708857

75. Finn, R. S., Merle, P., Granito, A., Huang, Y. H., Bodoky, G., Pracht, M., … Bruix, J. (2018). Outcomes of sequential treatment with sorafenib followed by regorafenib for HCC: Additional analyses from the phase III RESORCE trial. *Journal of hepatology*, *69*(2), 353–358. doi:10.1016/j.jhep.2018.04.010

76. Finn, R. S., Merle, P., Granito, A., Huang, Y. H., Bodoky, G., Pracht, M., … Bruix, J. (2018). Outcomes of sequential treatment with sorafenib followed by regorafenib for HCC: Additional analyses from the phase III RESORCE trial. *Journal of hepatology*, *69*(2), 353–358. doi:10.1016/j.jhep.2018.04.010

77. Chen, H. C., Jeng, Y. M., Yuan, R. H., Hsu, H. C., & Chen, Y. L. (2012). SIRT1 promotes tumorigenesis and resistance to chemotherapy in hepatocellular carcinoma and its expression predicts poor prognosis. *Annals of surgical oncology*, *19*(6), 2011–2019. doi:10.1245/s10434-011-2159-4

78. Saxton, R. A., & Sabatini, D. M. (2017). mTOR Signaling in Growth, Metabolism, and Disease. *Cell*, *168*(6), 960–976. https://doi.org/10.1016/j.cell.2017.02.004

79. Kim DH, Sarbassov DD, Ali SM, King JE, Latek RR, Erdjument-Bromage H, Tempst P, Sabatini DM. mTOR interacts with raptor to form a nutrient-sensitive complex that signals to the cell growth machinery. Cell. 2002;110:163–175

80. Hara K, Maruki Y, Long X, Yoshino K, Oshiro N, Hidayat S, Tokunaga C, Avruch J, Yonezawa K. Raptor, a binding partner of target of rapamycin (TOR), mediates TOR action. Cell. 2002;110:177–189

81. Kim DH, Sarbassov DD, Ali SM, Latek RR, Guntur KV, Erdjument-Bromage H, Tempst P, Sabatini DM. GbetaL, a positive regulator of the rapamycin-sensitive pathway required

for the nutrient-sensitive interaction between raptor and mTOR. Molecular cell. 2003;11:895–904

82. Jacinto E, Loewith R, Schmidt A, Lin S, Ruegg MA, Hall A, Hall MN. Mammalian TOR complex 2 controls the actin cytoskeleton and is rapamycin insensitive. Nature cell biology. 2004;6:1122–1128

83. Fountain, John H. (5 May 2019). "Physiology, Renin-angiotensin system" *NCBI*. NIH. Retrieved 29 Feb 2020

84. Szklarczyk D, Gable AL, Lyon D, Junge A, Wyder S, Huerta-Cepas J, Simonovic M, Doncheva NT, Morris JH, Bork P, Jensen LJ, von Mering C.
STRING v11: protein-protein association networks with increased coverage, supporting functional discovery in genome-wide experimental datasets.
Nucleic Acids Res. 2019 Jan; 47:D607-61

85. Petrov, A. S., Gulen, B., Norris, A. M., Kovacs, N. A., Bernier, C. R., Lanier, K. A., Fox, G. E., Harvey, S. C., Wartell, R. M., Hud, N. V., & Williams, L. D. (2015). History of the ribosome and the origin of translation. *Proceedings of the National Academy of Sciences of the United States of America*, *112*(50), 15396–15401. https://doi.org/10.1073/pnas.1509761112
86. Fox G. E. (2010). Origin and evolution of the ribosome. *Cold Spring Harbor perspectives in biology*, *2*(9), a003483. https://doi.org/10.1101/cshperspect.a003483

87. Genuth, N. R., & Barna, M. (2018). The Discovery of Ribosome Heterogeneity and Its Implications for Gene Regulation and Organismal Life. *Molecular cell*, *71*(3), 364–374. https://doi.org/10.1016/j.molcel.2018.07.018

88. Watanabe, H., Inaba, Y., Kimura, K. *et al.* Sirt2 facilitates hepatic glucose uptake by deacetylating glucokinase regulatory protein. *Nat Commun* **9,** 30 (2018). https://doi.org/10.1038/s41467-017-02537-6

89. Chen, J., Chan, A.W., To, K.-F., Chen, W., Zhang, Z., Ren, J., Song, C., Cheung, Y.-S., Lai, P.B., Cheng, S.-H., Ng, M.H., Huang, A. and Ko, B.C. (2013), SIRT2 overexpression in hepatocellular carcinoma mediates epithelial to mesenchymal transition by protein kinase B/glycogen synthase kinase-3β/β-catenin signaling. Hepatology, 57: 2287-2298. doi:10.1002/hep.26278

90. Arteaga, M., Shang, N., Ding, X., Yong, S., Cotler, S. J., Denning, M. F., Shimamura, T., Breslin, P., Lüscher, B., & Qiu, W. (2016). Inhibition of SIRT2 suppresses hepatic fibrosis. *American journal of physiology. Gastrointestinal and liver physiology*, *310*(11), G1155–G1168. https://doi.org/10.1152/ajpgi.00271.2015
91. Gong, J., Yan, S., Yu, H., Zhang, W., & Zhang, D. (2018). Increased Expression of Lysine-Specific Demethylase 5B (KDM5B) Promotes Tumor Cell Growth in Hep3B Cells and is an Independent Prognostic Factor in Patients with Hepatocellular Carcinoma. *Medical science monitor : international medical journal of experimental and clinical research*, *24*, 7586–7594. https://doi.org/10.12659/MSM.910844

92. Zhang, Y., Chen, J., Wu, S. S., Lv, M. J., Yu, Y. S., Tang, Z. H., Chen, X. H., & Zang, G. Q. (2019). HOXA10 knockdown inhibits proliferation, induces cell cycle arrest and apoptosis in hepatocellular carcinoma cells through HDAC1. *Cancer management and research*, *11*, 7065–7076. https://doi.org/10.2147/CMAR.S199239

93. Liu, G., Zhou, L., Zhang, H., Chen, R., Zhang, Y., Li, L., Lu, J. Y., Jiang, H., Liu, D., Qi, S., Jiang, Y. M., Yin, K., Xie, Z., Shi, Y., Liu, Y., Cao, X., Chen, Y. X., Zou, D., & Zhang, W. J. (2017). Regulation of hepatic lipogenesis by the zinc finger protein Zbtb20. *Nature communications*, *8*, 14824. https://doi.org/10.1038/ncomms14824

94. Kim, K., Boo, K., Yu, Y.S. *et al.* RORα controls hepatic lipid homeostasis via negative regulation of PPARγ transcriptional network. *Nat Commun* **8,** 162 (2017). https://doi.org/10.1038/s41467-017-00215-1

95. Ma, L., Robinson, L. N., & Towle, H. C. (2006). ChREBP•Mlx Is the Principal Mediator of Glucose-induced Gene Expression in the Liver. *Journal of Biological Chemistry*, *281*(39), 28721–28730. doi: 10.1074/jbc.m601576200

96. Liberzon, A., Birger, C., Thorvaldsdóttir, H., Ghandi, M., Mesirov, J. P., & Tamayo, P. (2015). The Molecular Signatures Database (MSigDB) hallmark gene set collection. *Cell systems*, *1*(6), 417–425. https://doi.org/10.1016/j.cels.2015.12.004

97. Knebel B, Haas J, Hartwig S, Jacob S, Köllmer C, Nitzgen U, et al. (2012) Liver-Specific Expression of Transcriptionally Active SREBP-1c Is Associated with Fatty Liver and Increased Visceral Fat Mass. PLoS ONE 7(2): e31812. https://doi.org/10.1371/journal.pone.0031812